An Examination of Close-Range Photogrammetry and Traditional Cave Survey Methods for Terrestrial and Underwater Caves for 3-Dimensional Mapping

by

Trey Olen Lee

A Thesis Presented to the
Faculty of the USC Graduate School
University of Southern California
In Partial Fulfillment of the
Requirements for the Degree
Master of Science
(Geographic Information Science and Technology)

December 2018

Dedicated to Alexey, for always being there for me and encouraging me to further my education,

And to Cody, whose continuous support and friendship will forever be greatly appreciated.

Table of Contents

List of Figures

List of Tables

Acknowledgments

There are many people who contributed and made this thesis possible. First and foremost, I want to thank my dive team for risking their lives in the name of science and for having to put up with me for long weeks in Quintana Roo. Stephen Daire welcomed me to his team of graduate students to begin research into the cenotes and other marine projects after working together on a project on Catalina Island, and my life has not been the same since. He and Emery Nolasco contributed their own personal funds for our preliminary survey in August 2017, and they have both helped me grow as a researcher and as a diver.

Jeronimo Avilez is one of the leading underwater archaeologists in Quintana Roo, and he was kind enough to offer our team a place to set up office and work out of. He showed us many of his findings and taught us about the history of the area and how he is using photogrammetry in his current work. His mentorship and willingness to help are just some of the great qualities about him and I hope I get the opportunity to worth with more scientists like him.

Colton Flynn, Garrett Quinby, and Cody Pilgreen made the terrestrial cave survey for this study possible. Their eagerness to learn and impeccable teamwork made the terrestrial portion fun and adventuresome, and I could not have asked for a better team to work with. Christine Loew spent several days diving Cenote Taj Mahal to acquire the data I requested for the underwater portion of this study, and there were many lessons learned thanks to her tireless effort. I am also grateful to the people from Alabaster Caverns State Park for being so welcoming and providing our permits without charge.

I have thoroughly enjoyed the program at USC, and each of my professor's teachings contributed to how this thesis was designed and carried out. Dr. Loyola, my thesis advisor, has been vital to keeping me on track and has provided guidance throughout every turn. Her

suggestions helped fix many flaws in my original plans and I could not have asked for a more supportive faculty member to advise me. I am also grateful to Dr. Ginsburg and Dr. Fleming for taking time out of their busy schedules to provide guidance and help tackle the issues faced.

List of Abbreviations

AAUS	American Academy of Underwater Sciences
AR	Augmented reality
BCRA	British Cave Research Association
CRP	Close-range photogrammetry
FOV	Field of view
GCP	Ground control point
GIS	Geographic information system
GISci	Geographic information science
GPS	Global positioning system
HMD	Head-mounted display
LiDAR	Light detection and ranging
PADI	Professional Association of Diving Instructors
SfM	Structure from motion
TDI	Technical Diving International
TLS	Terrestrial laser scanning
UAV	Unmanned aerial vehicle
USC	University of Southern California
VR	Virtual reality

Abstract

Caves historically have been one of the most difficult types of terrain for mapping and data acquisition due to the inability to use satellites, aerial imagery, or even accurate GPS receivers. Karst science typically relies on outdated survey methods, but advances in technology which allow for 3D models of terrestrial objects and terrain, are slowly making their way into Karst science. The most accurate method of remotely scanning areas and collecting accurate data, light detection and ranging (LiDAR) produces impressive and accurate 3D models and even detects sub-canopy elevation changes. However, its prohibitive costs and processing requirements make it unavailable to many. Close-range photogrammetry (CRP) is an affordable alternative given cost, but at the loss of accuracy in the 3D model produced.

While CRP with geo-referenced imagery can be used to produce 3D models of terrestrial landscapes and objects or "floating" subterranean objects, there are few studies that have utilized CRP in the entirety of an enclosed cave environment. This study examines a previous methodology used to create 3D models of terrestrial caves as a way to model underwater cave systems as well as terrestrial systems. The aim is to validate this methodology and apply it to different systems, with minor necessary adjustments. The photogrammetry data collection process utilized a GoPro Hero 5 camera and floodlights to collect imagery, which were processed using Agisoft PhotoScan Professional. High accuracy GPS receivers were used to collect cave entry coordinates to produce georeferenced models that were imported into ArcGIS. Traditional surveys were conducted to compare models. The methodology requires further modification and technical diver training to produce 3D models successfully of underwater cave systems via photogrammetry. Using a modified version of Jordan's (2017) methodology produced promising results and 3D models of the terrestrial caves.

Chapter 1 Introduction

Cave systems offer unique challenges with regards to spatial data acquisition, particularly the lack of global positioning system (GPS) receiver capabilities. Caves can appear in many different forms and variations, some of which cause the cave to be partially or completely underwater. Many of the world's terrestrial caves have been explored and mapped through traditional survey methods, but there are many underwater caves being discovered in the southeastern region of Mexico and many caves that are not yet mapped. The unnerving darkness and limited air supply of underwater caves add to the already arduous task of data acquisition. Modern technology allows scientists to collect data on the multiplanar aspect of caves and map them in a 3-Dimensional (3D) format. These types of data can help a wide range of scientists, from biologists marking the locations of rare cave-adapted organisms to environmental scientists determining potential sources of pollution. A map, whether 2D or 3D, is the fundamental piece of the puzzle to start with. High quality maps can also help explorers adequately plan their expedition, taking into account how much climbing and swimming may be required. 3D cave data can help predict areas likely to flood and may indicate passages that should be avoided during heavy precipitation. More cave divers are switching their configuration from the traditional backmount to sidemount, which positions two air tanks to the side of the diver at hip level. This allows a diver to squeeze through tighter passages without damaging the caves and it greatly reduces the risk of bumping an air tank on the overhead and causing it to leak. Despite this shift toward side mount, many divers continue to dive caves with a standard single-tank configuration. For divers, the ability to measure the height and width of passages in a 3D model could prevent a diver from becoming stuck in a passage that is too small for that diver's equipment configuration.

Many scientists have been using light detection and ranging (LiDAR) to create 3D maps and models of both terrestrial and aquatic caves and the objects within them. However, the high cost of LiDAR scanners can be prohibitive for projects without large budgets. And though production costs of these sensors are beginning to drop, submersible LiDAR scanners with a range of more than a few meters remain above $100,000. As a result, the methods of terrestrial cave data acquisition have been evolving faster than its marine counterpart. Underwater cave mapping still relies on traditional methods of underwater surveying and outdated tools, such as knotted rope for measuring distance and a dive slate to sketch the estimated distance of walls from the survey line, which only produce 2D models. In lieu of LiDAR, close-range photogrammetry (CRP) is a proposed low-cost solution for creating georeferenced 3D models from a collection of overlapping photographs. Additionally, CRP can be performed in both terrestrial and aquatic environments and by georeferencing the models, they can be used within a geographic information system (GIS) to conduct spatial analyses. There are many cases like the mapping of the Maya landscape in Caracol, Belize (Chase et al. 2010) where LiDAR works great for discovering features underneath forest canopy, but the resolution is too low for usable 3D models and only the tops of features are included. This research was expanded in 2016 by the Pacunam LiDAR Initiative (PLI) by surveying a total of 2144 km² in Guatemala (Canuto et al. 2018). This was the largest LiDAR survey to date and the results showed 61,480 structures with a density at 29 structures/km², which is much higher than previously thought. It is possible that on the ground CRP can be added to LiDAR data collection in these heavily canopied areas to create 3D models.

The methods described in this document can potentially be extended to other environments where GPS and satellite/UAV imagery are not possible, such as extremely dense

forests with an impenetrable canopy. The purpose of the study presented here is to validate previous methods (Jordan 2017) used to develop 3D models of terrestrial caves and test CRP in an underwater cave system.

It should be noted that anyone wanting to attempt spelunking or cave diving should have the proper training, experience, and equipment before venturing into such a hazardous environment. Cave diving is dangerous for even the most qualified divers and, as with all dives, should include the use of a dive buddy for safety purposes. This study included several experienced members of a dive team for the underwater cave survey as well as a team of graduate students for the terrestrial cave survey.

1.1. Cenotes: The Maya Underworld

In many parts of the world, vast networks of underground cave systems exist that can stretch for anywhere from a few meters to several kilometers. The Yucatan peninsula in Mexico is a prime example, where above ground there are thousands of cenotes, commonly known as sinkholes, throughout the region. These cenotes have been a precious source of groundwater for thousands of years and played a significant role in the Maya civilization and their religious practices (Lopez 2008). Cenotes also functioned as holy spaces for rainmaking rituals and ceremonies associated with concepts of life, death, rebirth, and fertility. The Mayas viewed the cenotes as gateways to Xibalba, which roughly translates to “place of fear,” the underworld realm ruled by the Maya death gods. This is one of the reasons human remains and artifacts are often found inside the cenotes. Even before the Maya use of cenotes, early humans used these cave systems for shelter (Gonzalez et al. 2014).

One prominent issue with these cave systems is that only a small percentage have been formally mapped. The Quintana Roo Speleological Survey maintains an archive of cave survey

data for more than 358 underwater caves (Quintana Roo Speleological Survey 2018), a small amount in comparison to the thousands of cenotes that have been discovered over the years. Without proper mapping of these below ground systems, people unknowingly have built homes and buildings on top of structurally unsound caverns. This does not always present a problem, but there is the risk of the limestone collapsing and plunging the building and its content into the depths many meters below.

Another topic of concern is the archaeological/anthropological significance of these cenotes, which contain evidence of the first American settlers and fossils of prehistoric animals (Gonzalez et al. 2014). Because the cenotes have become a popular tourist attraction, many artifacts are being stolen by "treasure hunting" sport divers. This has led to a sense of urgency among archaeologists to recover artifacts before they are stolen. While the extent of the cenotes should be publicly available, the locations of artifacts within them must also be protected. The exact coordinates of the artifacts can be collected before removal to allow for accurate digital recreations of a site. This allows the artifacts to be preserved while also allowing for spatial analysis of a scene later.

Although the cenotes also contain a source of fresh groundwater that has been used for thousands of years, in recent years some of them have been polluted with sewage from nearby towns. There is concern among scientists of the environmental impact of this pollution. Specialists have concluded that the cenotes are systems at risk and, consequently, that the scientific potential is also endangered (Lopez 2008). By mapping these cenotes using georeferenced models and advanced GIS analysis and modeling, we may be able to aid in identifying unknown sources of pollution and assess areas that might be at risk of contamination.

While beaches provide color-coded warning flags when the risk of rip tides or swells is high, there is no system of warnings for potentially dangerous dive areas. Most underwater caves merely have a sign at the entrance that tells people to turn around, and admittedly, some divers ignore the signage, which is especially dangerous because some cave systems are more complex than others are. With accurate maps, a diver can discern if a particular site is within his or her level of training and comfort and be better prepared when entering the cave system. The general rule for cave divers is to turn around when one member of the dive team uses 1/3 of his or her air supply, but a dive team may decide to turn around at an earlier point if a cave has many interconnecting passages that could cause a diver to become lost if line markers somehow are removed. Additionally, scientific divers and archaeologists have tasks to perform outside of navigating, such as sample collection, so having easily understood maps can aid in their planning process to reduce the risk of accidents or death.

1.2. Traditional Underwater Cave Surveying

The ability to explore and document underwater caves has become possible with the advancements of scuba diving technology during the last century. However, the tools and methods used today cannot keep up with the advancements in terrestrial surveying (see Section 1.3). Underwater cave surveying relies on methodologies such as line-of-sight measurements and geometric calculations between survey stations and are difficult and time-consuming to obtain (Hunt et al. 1987). Traditionally, caves are surveyed using a knotted rope, compass, pencil, and paper. However, pencil and paper will not work underwater, so a dive slate is substituted. It is a lot of equipment to carry, but it can be even more daunting when adding in the need for a flashlight and maintaining proper buoyancy with all the tasks of cave diving. Once a survey is complete, it can be assigned a survey grade based on accuracy of measurements and in cave

sketches. The survey grade standards set by the British Cave Research Association that apply to both terrestrial caves and underwater caves include seven grades and four classes (*BCRA Survey Grades* 2002). Table 1 below shows how the survey grading system is set up. The surveys conducted for this study meet Grade 4 and classes are not included in the table because no sketching was performed for this study. The terrestrial surveys were conducted while the bats were not hibernating in the caves, but there was contact with aquatic organisms in the cenote where precautions had to be taken. As is the case when working in any environment with wildlife, there are many factors to consider when conducting underwater cave surveys. Each location poses its own challenges and rewards; one specific and inherent environmental challenge is discussed below.

Table 1: Cave survey grades

Grade	**Description**
1	Sketch – Low accuracy – All measurements estimated, usually after leaving the cave
2	Higher grade sketch than Grade 1, but less than Grade 3 – Approximated measurements taken while in the cave
3	Magnetic survey – Angles measured ± 2.5 degrees – Distances measured ± 50cm or ± 1 2/3 ft.
4	Higher grade survey than Grade 3, but less than Grade 5
5	Magnetic survey – Angles measured ± 1 degree – Distances measured ± 10cm or ± 1/3 ft.
6	More accurate than Grade 5, or an attempt at grade X that failed to meet the requirements – All compass bearing and clinometer readings made to ± 0.5 degrees or less
X	Measurements taken using theodolites or similar using extremely accurate compass/clinometer on fixed stands

1.2.1. Effects on Aquatic Life

There is one potential area of concern regarding divers entering the cenotes. The species of fish *Astyanax mexicanus*, also known as the Mexican tetra, has been known to follow divers'

lights into the caves. Once in the caves, the fish feed on rare cave-adapted crustaceans. After asking divers local to Quintana Roo, it was discovered that there is a survey being conducted by CaveBiology about the behavior of these fish as observed by divers, but the results have not been published yet. As shown in Figure 1, a unique feature of these fish is that they appear in two different forms: cavefish and surface fish (Panaram and Borowsky 2005). The cave form has very little pigmentation in its skin, but the most notable aspect is the missing eyes. The cave form has a heightened sense of smell and its head is covered in taste buds. They also are able to store more energy as fat to go longer periods without eating. Despite their lack of eyes, *Astyanax* cavefish have retained the ability both to sense light and to alter their locomotor activity in response to photic stimulus, likely thanks to the pineal gland (Carlson & Gross 2018). To reduce the potential impact on both the cavefish and surface fish, it is recommended to turn on the dive lights only once inside the cave. This study abided by that recommendation to prevent the surface fish from following the diver into the caves to avoid disturbing the aquatic life of the cenotes. There was sufficient natural light outside for photogrammetry before the caves were entered.

Figure 1: Cave form (front) next to surface form (back two) (Credit: Richard Borowsky)

1.3. Terrestrial Cave Surveying

Standard areas of the earth can be mapped with satellites/unmanned aerial vehicles (UAVs) and specific points of interest can be measured with handheld GPS units, but these methods do not work for environments with overhead obstructions and enclosed cave systems. One method commonly used for terrestrial cave mapping is to collect GPS coordinates outside a cave and then use a tape measure, compass, and clinometer to measure distances and direction to survey stations set up throughout the cave. Each station must have a line of sight to the previous station as well as the following station. Once measurements are completed to the final station, they are usually measured in reverse to double check the accuracy. This network of line measurements is called a traverse, and it is what surveyors use to create a line map of an enclosed cave. The line map is used until the outer edges can be mapped and a more detailed interior map produced. Surveyors will often collect the left, right, up, and down (LRUD) distances to the walls at each station to aid in drawing an interpretation of the wall passages. In recent years, LiDAR scanning has been implemented in cave surveying by some scientists. 3D models produced by LiDAR scans have provided new methods to analyze the geomorphology of caves that expand upon the 2D methods traditionally used (Gallay et al. 2016). Figure 2 is one of the models of Domica Cave in Slovakia generated using laser scanners by Gallay and his team. However, although LiDAR scanners provide much higher resolution and accuracy, they are significantly more expensive than cameras used for photogrammetry.

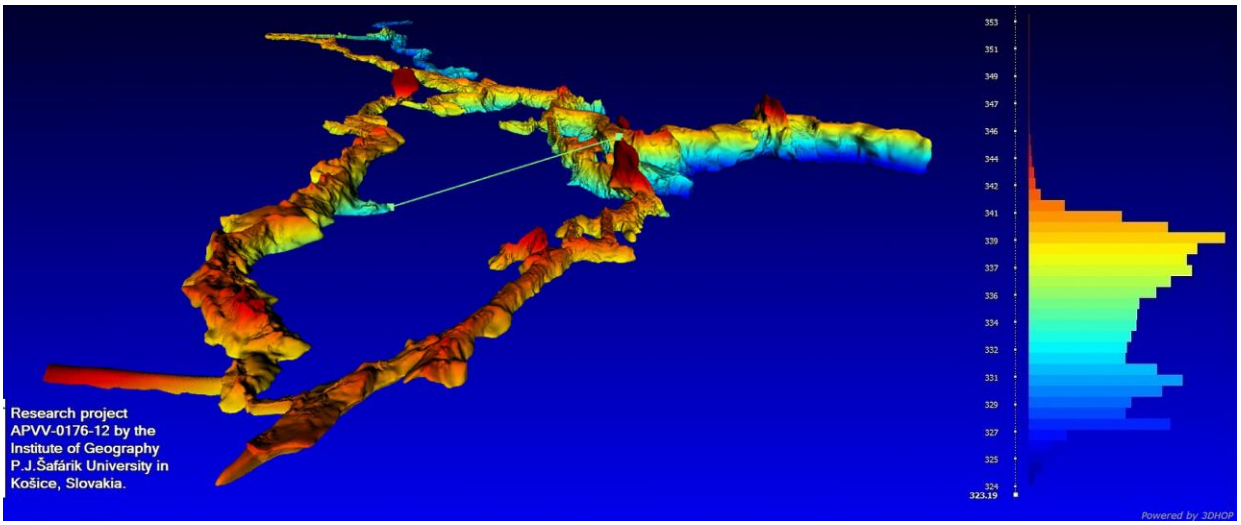

Figure 2: Domica Cave, Slovakia

As is the case when working in any environment with wildlife, there are many factors to consider when conducting terrestrial cave surveys. Each location poses its own challenges and rewards, a few of the inherent environmental challenges of terrestrial cave systems are discussed below.

1.3.1. White Nose Syndrome (WNS)

Terrestrial caves are prime bat habitats and many caves offer the opportunity to see entire colonies of bats (whitenosesyndrome.org 2018). While they may be known for carrying and transmitting rabies through their bites to humans, bats are also susceptible to a variety of diseases that can be carried and transmitted by humans to bats. An agent, Pseudogymnoascus destructans, a psychrophilic fungus that infects the skin of bats and leads to depletion of their fat stores during hibernation (Griggs et al. 2012) causes one of these diseases, White Nose Syndrome (WNS). It gets its name from the way the affected bat's nose looks, as if it is covered with a white fuzz. WNS was first discovered in 2006 near Albany, New York, and it has since spread as far as Quebec and North Carolina with some isolated reports in Oklahoma and Missouri (Cohn

2012). Because WNS affects hibernating bat populations, extra precautions must be taken to not transmit this disease to them. It is considered one of the worst wildlife diseases in modern times, having reduced the little brown bat population by more than 90 percent. Figure 3 below shows how WNS has been spreading across the United States. There are strict decontamination procedures in place for caving equipment to prevent the spread of WNS, if a caver does come into contact with the disease. Therefore, the terrestrial site for this thesis was carefully chosen to avoid encountering WNS.

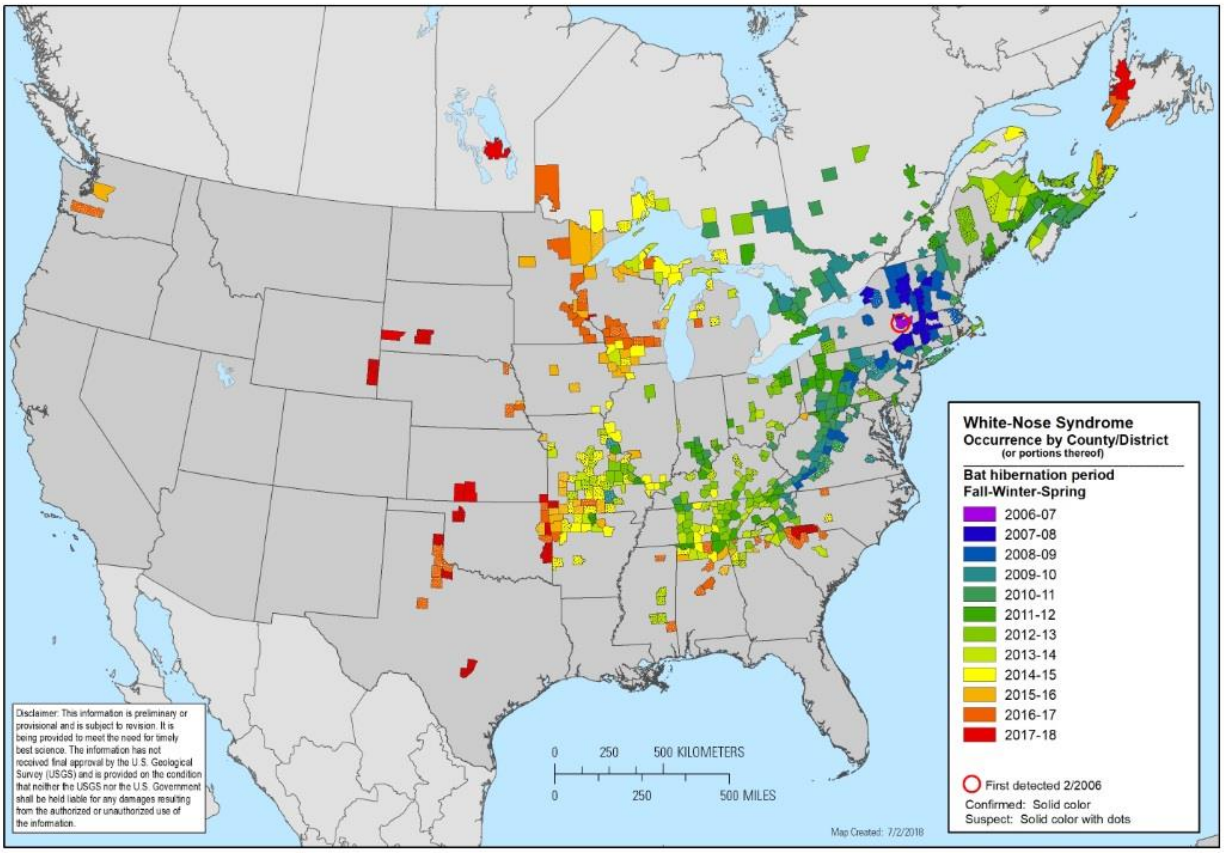

Figure 3: WNS occurrence map. Available at https://www.whitenosesyndrome.org/resources/map.

1.3.2. Cave Accidents and Deaths

There was little research into caving accidents conducted before 2009, when a man named John Jones tragically died in a caving accident in Utah. Jones and 10 other friends and family members explored Nutty Putty Cave just before Thanksgiving. Nutty Putty Cave is considered a beginner's cave, but there are sections where people have required rescue in the past. Jones became stuck upside down after crawling through an 18-by-10-inch L-shaped bend. Rescue crews worked for more than 24 hours before Jones lost consciousness and died (Spring 2012).

The accident sparked the beginning of research conducted by the University of Virginia Medical School that examined past incidents. During their 28-year study period, there were roughly 50 caving accident victims reported each year on average (Stella-Watts et al. 2012). This is more than three times the number of shark attacks reported each year in the United States, and that number does not include cave diving accidents.

Extra precautions were taken during this study to ensure proper briefing on cave team assembly and cave knowledge. Every team member wore a hardhat equipped with a light, two backup flashlights, boots, long sleeves, and jeans. There was also food, water, and a first aid kit on hand. Two of the team members were certified in Emergency First Response.

1.4. Photogrammetry

One method people use to create a 3D model of an object or space is with photogrammetry. Photogrammetry is formally defined as the art, science, and technology of obtaining reliable information about physical objects and the environment through the process of recording, measuring, and interpreting photographic images and patterns of electromagnetic radiant energy and other phenomena (Matthews 2008). In other words, photogrammetry uses

georeferenced photos to build an object or environment. The main advantage to using photogrammetry is the low cost and skill involved in its use compared to LiDAR scanning. Photogrammetry can be classified into two categories: aerial and close-range, both are discussed below. This study will evaluate if CRP is a viable method for underwater cave data acquisition and validate the method used in terrestrial cave data acquisition by Jordan (2017).

1.4.1. Aerial Photogrammetry

Aerial photogrammetry uses imagery collected from sources such as unmanned aerial vehicles (UAVs), airplanes, and satellites. The operator typically collects the imagery at a 45-degree angle and goes in a snake pattern to acquire overlapping photographs that cover the entire project area. A variety of products can be derived from the use of photogrammetry, including digital terrain models (DTMs), orthophotos, and vector maps (Matthews 2008). A DTM is a digital representation of the earth's surface, but it can also be called a digital elevation model (DEM) or a digital surface model (DSM) depending on the exact information it is representing. An orthophoto corrects distortions and differences in scale from the effects of camera tilt and relief displacement. Essentially, an orthophoto represents the terrain from a top-down view and can be used as a map on which to overlay other information. Finally, vector maps allow for the digitization of points, lines, and polygons of areas of interest using real-world coordinates.

1.4.2. Close-Range Photogrammetry (CRP)

On the opposite end of the spectrum, close-range photogrammetry gets much closer to the objects being modeled. The use of imagery collected with a camera-to-object distance of less than 300 m is considered close-range photogrammetry (Matthews 2008). Typically, CRP is used to create 3D models of individual objects such as statues or walls with distinct features, but CRP can also be extended to room-scale applications. CRP can establish cave passage walls, ledges,

profiles, and cross-sections more accurately than the traditional methods of sketching (Jordan 2017).

1.5. Georeferencing

Georeferencing is the process of associating points in non-spatial imagery with points tied to a coordinate system. This can be a local coordinate system used for a specific project or it can be a geographic or projected coordinate system where the points are tied to real-world locations. The purpose of georeferencing is to allow a geographic information system (GIS) to perform spatial analyses on data that otherwise would not be possible. The sparse point cloud is the most basic form of the 3D model that is built using matching points from imagery. The matching points in the imagery are what produce the point cloud during the alignment process. The sparse cloud is expanded into a dense cloud with a higher number of points, which is then used to create the surface, or mesh, of a 3D model. When a 3D model is georeferenced, a DEM can be built using the data from the sparse cloud, dense cloud or mesh. The mesh can be built directly from the sparse cloud to save processing time, but the accuracy and resolution suffers as a result. The resolution of the DEM is directly related to the source data, where a higher number of points or triangles will lead to a higher resolution.

There are two traditional methods for georeferencing a point cloud: direct and indirect (Santos 2013). The direct method involves using additional sensors such as a GPS and an inertial measurement unit (IMU). The indirect method involves the measurement of control lines derived by segmenting and intersecting two adjacent planes that are not parallel. The georeferencing method described here involves the measurement of points outside the cave at ground surface level with a GPS unit and then using a program called Forward3D with the azimuth, altitude, and target-to-target distance to calculate the real world coordinates of ground

control points (GCPs) inside a cave. The coded targets in Figure 4 served as the GCPs and doubled as scale bars in both cave systems. Forward3D works exclusively on the GRS80 ellipsoid. It should be noted that GRS80 and WGS84 are essentially the same with only a very minor variation in the semi-minor axis. This variation would cause a shift in data by approximately a few meters depending on the site's location, but the positional accuracy needs of this study are not precise enough for it to affect it. There is also the option to use the Bearing Distance to Line tool within ArcGIS Pro to calculate the coordinates of the GCPs, but it should be noted that it is important to use the ellipsoidal distance instead of the target-to-target distance because although the difference is minor in small-scale projects, the accuracy will decrease as distance increases. Jordan (2017) calculated x, y, and z values based on azimuth and zenith from the starting point (Figure 5). Forward3D uses the same values to calculate ΔX and ΔY, and the ΔZ formula was used within Microsoft Excel.

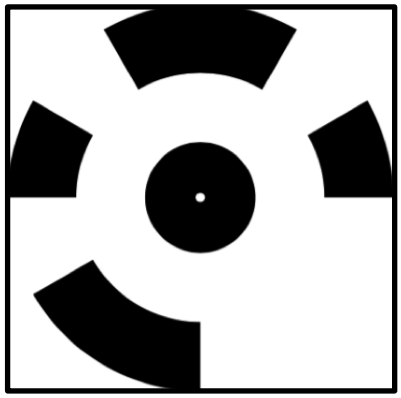

Figure 4: Unique coded photogrammetry targets recognized by Agisoft PhotoScan

$$\Delta X = [R*\cos(\zeta)]*\cos(\alpha)$$

$$\Delta Y = [R*\cos(\zeta)]*\sin(\alpha)$$

$$\Delta Z = R*\sin(\zeta)$$

Figure 5: Formula used by Jordan (2017) where R is distance between the stations, ζ is zenith value in radians, and α is azimuth value in radians

1.6. Thesis Organization

Photogrammetry has been used for many different applications and Chapter 2 summarizes such related scenarios involving photogrammetry and 3D models. Chapter 3

describes the methods and materials used for this study, along with methodological considerations and exceptions made from Jordan's (2017) original research. Chapter 4 looks at the results from Taj Mahal, Ice Cave, and Owl Cave. The results consist of how the survey data were used along with the photogrammetry to create additional outputs such as full and internal DEMs and georeferenced 3D models. The closing chapter analyzes the obstacles that were faced throughout this study, the steps that were taken to reduce error, and my personal thoughts on how to expand this subject further.

Chapter 2 Related Works

This chapter reviews the previous thesis (Jordan 2017) that this study is based on in section 2.1. To give a broader perspective on photogrammetry and 3D models, this chapter also reviews similar studies on terrestrial laser scanning combined with photogrammetry and interior 3D scanning. Lastly, this chapter covers different photogrammetry software and how the final model outputs can be used.

The data acquisition methods described in this study have been established in many applications including terrestrial caves but utilizing them in underwater caves is a concept that has not been researched in depth. There are few studies of these methods being used in cave environments, and even fewer in underwater cave environments. The principles used in terrestrial cave surveying can be carried over to underwater cave surveying with a few adjustments, considering the limitations imposed by being underwater. An example of practical use of photogrammetry in caves is the recording of ancient cave paintings in Malaysia. Originally, the archaeologists at the Department of Heritage Malaysia used tracing paper and photography to record the paintings, but the tracing paper is exposed to damage and the recorded paintings are out of scale (Majid et al. 2017). The difficult part of recording the paintings is the multi-planar features of them. Both photogrammetry and laser scanning are now being used for non-contact mapping and recording of these paintings. The results from both were remarkably similar and geometrically accurate. The cenotes are archaeologically/anthropologically significant just like the cave paintings in Malaysia, so it is important to be able to document them with spatial accuracy.

2.1. Photogrammetry in Caves

Photogrammetry provides detailed, photo-realistic 3D models that include unique features that are needed in cave models. The use of photogrammetry requires a series of well-lit photographs to create a point cloud. These photographs must overlap each other by at least 60% to be effective (Matthews 2008). Some caves will have enough natural light to suffice, but there will almost always be areas with little or no light. One proposed methodology to use in caves (Jordan 2017) goes against many rules of thumb in photogrammetry by operating in the dark with a moving flood light and the use of a wide-angle fish-eye lens. The moving light source only becomes an issue if the operator is not careful about the casting of harsh shadows into the field of view of the camera. Jordan (2017), in his study of Arkansas caves, used a GoPro camera with a 1000 lumen flood light to create photogrammetric models of terrestrial caves. If a 1000 lumen light was sufficient in terrestrial caves, it is safe to assume a more powerful light will be required underwater. The photogrammetry software used in Jordan's research was Agisoft Photoscan, in order to maximize the replicability of the validation study, the same software is used in this study.

Jordan (2017) outlines several workflows throughout his study that offer a baseline to improve upon. He used ArcGIS to convert the raster data from the photogrammetry models into vector data, and then applied a positive and negative buffer to create the basic XY outline of a cave to compare to the traditional survey map. Wycisk (2016) used a local coordinate system for georeferencing an industrial mineral mine in Norway while Jordan (2017) used a projected coordinate system, which shows the viability of both options. For the purposes of this study, a geographic coordinate system was used because of the 3D nature of the models. This also allowed the models to be overlaid on a topographic map to show the extent of the cave's interiors

in relation to the surface. However, a projected coordinate system may be required for measurements that are more accurate. Various methods of acquiring cave imagery and building interior cave models are discussed below.

2.2. Still Photography and Video

Another proposed methodology used in a Norwegian mine (Wycisk 2016) involves the use of multiple stationary light sources that are placed on the same axis of the camera locations. The standard method of still photography was used by Wycisk in conjunction with multiple light sources. For specific circumstances in other studies, this method may be required in some areas due to the varying nature of caves and how far light travels underwater. Wycisk used the models produced by photogrammetry to show how every explosive blast changed the shape of a drift. A model was made before and after the first blast, then again after a second and third blast. Three models of the same drift are shown in Figure 6, where the drift has extruded further in each model. Model 1 is at the drift's earliest point in time while model 3 is the latest.

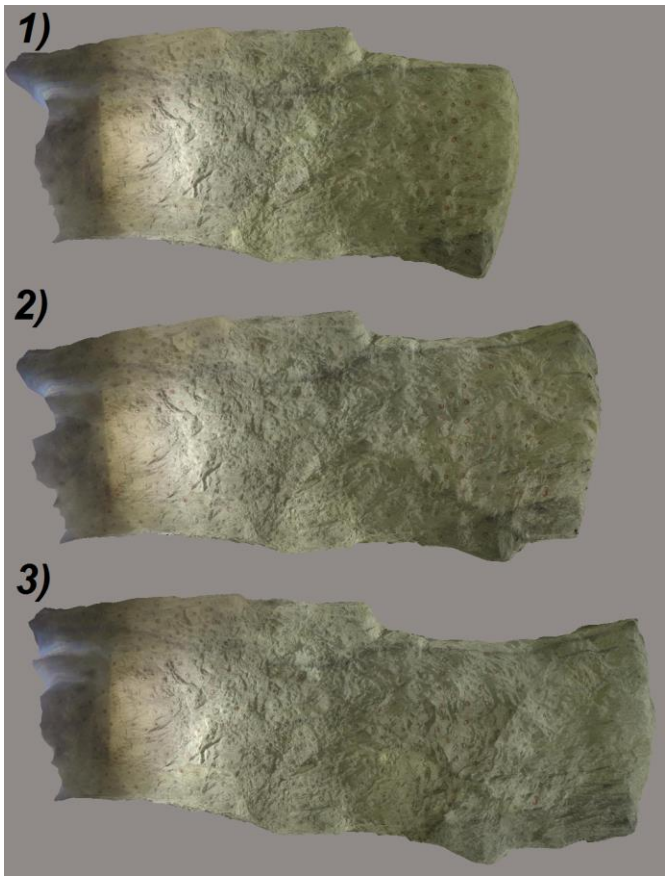

Figure 6: Photogrammetry models of a drift before and after two explosive blasts

In 2018, Agisoft released version 1.4 of PhotoScan, which includes the ability to import video directly instead of using outside software to capture still frames from video. Agisoft PhotoScan 1.4 allows the user to specify the framerate to pull still images from, where a lower framerate value will generate a higher number of images. These images are in PNG format instead of the JPEG format with which most people are familiar. The PNG format does not use the compression that is applied to JPEG's, which provides PhotoScan with more potential tie points between images. Traditionally, still photos are captured in RAW format to retain camera metadata. This camera and lens data is important because the software uses it to estimate the location of the camera at the time the photo was collected. Without the correct data, the

photogrammetry software will default to a typical lens (50mm) that would be used in photography. This may not cause problems with some projects, but a 50mm lens will almost never be used in underwater environments, as it will result in inaccurate camera location estimations. Once the PNG files are loaded, the camera and lens information needs to be manually entered.

The ability to use video drastically changes how a photogrammetry project can be approached. In underwater environments where time is limited to air supply, the stills-from-video approach allows a wider area to be scanned at the minor expense of reduced quality and a few extra steps in the post-processing of the imagery.

2.3. Terrestrial Laser Scanning Combined with Photogrammetry

Terrestrial laser scanning (TLS) is a highly accurate, but costly method to produce 3D models. Underwater laser scanners are even more expensive than terrestrial laser scanners. According to a sales rep at 2G Robotics, an industry leader in submersible laser scanners, one can cost as much as $100k for a scanner with more than a few meters range. Laser scanning and photogrammetry have opposite drawbacks and strengths, however. Accuracy is laser scanning's greatest strength, but the models lack photorealism. On the other hand, photogrammetry may not produce as accurate of a model, but it looks true to life because the model is built from photographs. If both technologies are used in synergy to create a 3D model, then laser scanning can create the accurate 3D model and photogrammetry can apply quality color information (Koska and Kremen 2013).

The process that Koska and Kremen (2013) used to model a large cathedral started with the creation of an accurate 3D polygonal model using the data from the laser scans from the Leica HDS3000 and Surphaser 25HSX. After the scan was completed, they used the structure from motion (SFM) method to collect the needed images with a Canon EOS 5D Mark II and a Sony NEX-5. Once the transformation of images from the SfM coordinate system to the 3D model coordinate system was completed, they optimized the image/texture mapping on the 3D model. The scanning density was set to reach 5 mm average point spacing throughout the model. Agisoft PhotoScan was the primary software used for the model of St. Nicholas Baroque Church (Figure 7). By following this approach, future research can use a laser scan of a cave that has a photogrammetric model for it and combine the two models. This process is not utilized in the current study because laser scans were not available for the sites.

Figure 7: 3D model mesh (left) and orthoimage (right) of St. Nicholas Baroque Church.

2.4. Interior 3D Scanning

Mapping landscapes and geography is a familiar subject to most in the Geographic Information Science (GISci) field, but the mapping of building interiors is one area of which we do not see much. It is an emerging challenge in architecture, but it is made more challenging by the lack of GPS functions inside indoor environments (Turner 2015). The mapping of the Boeing Jumbo 747-8, the world's longest airplane, is the perfect example of a complex interior mapping project that overcame some of these obstacles and was completed in just 18 hours (Industrial Product Finder 2013). The aircraft contained dozens of rows of seats and windows that all look alike and could be easily confused by photogrammetry software. Using two Creaform Handyscan 3D scanners, four scanning experts divided the plane into multiple sections to cover the entire aircraft in a time-efficient manner. They used scanners with an estimated accuracy of up to 0.040 mm and reflective targets that were positioned on the parts to be scanned. The project used a total of 5,000 targets, which is much greater than the number of targets required for this thesis and cave mapping in general.

Buildings and most other indoor environments are almost entirely planar, which allows the popular approach to fit only planar elements to the point clouds (Turner 2015). This also eliminates any obtrusions or objects not meant to be part of the final model. This plane-fitting method is further enhanced by analyzing the computed planes for holes in the surface, which would likely be the locations of doors and windows (Xiong et al. 2015). Two differences in cave scanning is that caves are not planar, and they do not have windows that would otherwise cause holes in the photogrammetry model, though they do have deep angles. The scanning method for a cave will vary slightly from a room scan depending on the geometry of the cave walls because

there may be formations blocking a camera path. This is discussed further in the next chapter, a detail of the methods and equipment that were used in this project.

2.5. Photogrammetry Software

Photogrammetry used to require an entire suite of different applications for each step of the process. Today, there are a multitude of software developers offering "all-in-one" packages for photogrammetry. Pix4D, RealityCapture, and Agisoft Photoscan are among the more popular options due to their accuracy and user-friendliness. There is much debate over which is the best option, and there are still many people who choose to run a photogrammetry model through separate applications for each step. For this study, Agisoft Photoscan Professional Edition (Ver. 1.4 2018) was utilized as the previous version of this software was used by Jordan (2017) in his study of the caves in Arkansas and also what the author has more experience with.

2.6. 3D Models and Their Uses

The models created in this study, and other studies like this, can benefit many disciplines, ranging from archaeology to urban planning. One example of a real-world company that uses 3D models of objects and environments every day is Bevel, located in Seattle, Washington. Bevel is a creative agency that partners with different enterprise clients to build immersive technology tools (Lee & Manning 2018). This can be something like building a virtual reality (VR) walkthrough of a hospital to aid with the design process or it can be a VR showcase of an upcoming high-rise for investors to verify what kind of view they can expect from any location in the building. Some people show a strong aversion to VR due to it being a closed-system, which is where augmented reality (AR) shows potential. Virtual reality requires the user to wear a head-mounted display (HMD) that fully-encloses the user's field-of-view (FOV). AR requires a similar HMD, but it allows the user to see what is in front of them and projects an image onto

the lenses that looks as if the object exists in the real word instead of solely in the digital one. For AR's features to appear correctly, they need to be georeferenced with either some form of GIS or with the use of fiducial markers, which act as references to "anchor" digital objects to the real world.

VR and 3D spatial analysis have received attention from military prospects, with promising results from studies. One study shows how a virtual simulation improved the live firing scores of students in a real world firing range (Bhagat et al. 2016). Students in that study were divided into four groups: the control group adopted only real world firing range didactics, experimental group 1 used only the VR firing range, experimental group 2 used only the VR combat training mode, and experimental group 3 used both the VR firing range and the VR combat training mode. Experimental group 3 showed significantly higher scores in the real world firing range when compared to the control group and the other experimental groups. 3D line-of-sight computation can also be performed in military simulations based on ray shooting (Auer and Zipf 2018). A ray is an incomplete line, represented by a start point and a direction. A ray can be tested to discover visible obstructions from any designated point, which can aid in choosing appropriate routes and places to stop.

Chapter 3 Methods and Materials

This chapter discusses the methodology used in both the underwater cave data acquisition and terrestrial cave data acquisition. Jordan's (2017) methodology was modified in different ways for each environment. Workflows for each are detailed, as well as the equipment and software used to produce the 3D models via photogrammetry. Georeferencing was a more involved task than simply using a GPS unit to collect coordinates at various points, and the formulas and calculations used here are described in section 3.5. The chapter concludes with the types of outputs to be expected in the results chapter.

To follow USC's guidelines on scientific diving, Christine Loew was contracted to perform the underwater data collection for this study. Christine is a world-renowned cave diver and instructor, with nearly 6,000 dives recorded in her dive log. Having no prior experience with photogrammetry or GIS, Christine was taught the basic principles of photogrammetry on land before the dives commenced.

3.1. Study Sites

The three caves in this study were selected based on their location, traffic, and geometry. The terrestrial caves are located in Alabaster Caverns State Park, which is the closest set of caves to the author that is publicly accessible. Cenote Taj Mahal is also publicly accessible, if the explorer has a valid cave diver certification card. A local guide must also accompany anybody who wishes to go cave diving in Quintana Roo. These rules were set in place to protect both divers and the caves from harm. The study sites and survey maps used for this study are shown in Figure 8 below. All three maps were analog to begin with, and were scanned and digitized using Adobe Illustrator, which eliminated unnecessary information and noise.

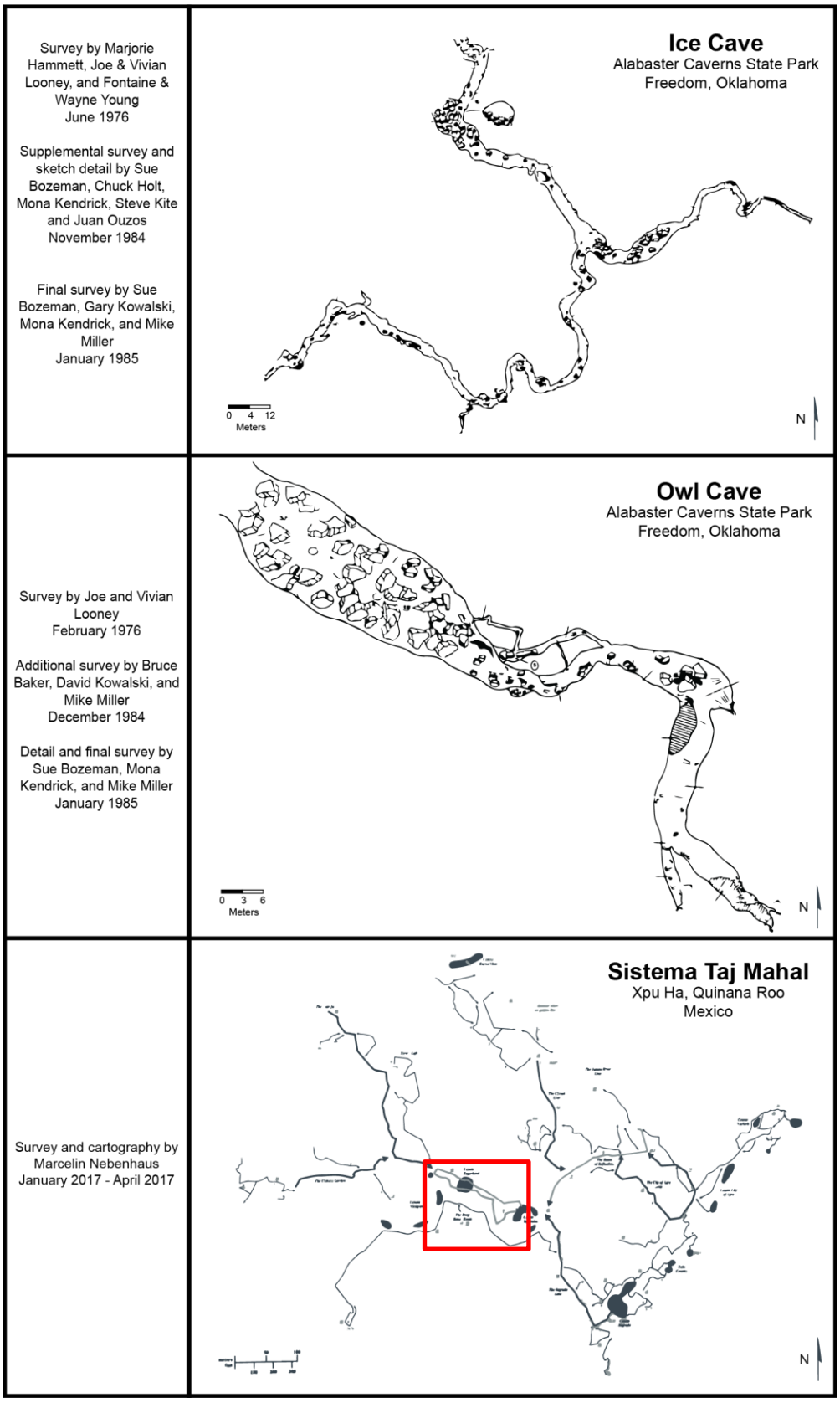

Figure 8: Traditional survey maps of sites used in this study

3.2. Data Description

There are several types of data listed in Tables 2 and 3 required for this study, some were acquired as raster files and others were collected *in situ*. Control maps for both the terrestrial and underwater caves were available from previous surveyors. The line survey, imagery, and GPS coordinates were all collected specifically for this study, and the coordinates for the GCP's were calculated.

Table 2: Underwater cave data requirements

Content	**Format**	**Description**
Line survey	CSV	Traverse data
Video footage	MP4	4K and 30fps
GCP coordinates	CSV	Calculated based on collected coordinates outside the cave
Control maps	Analog	Maps from Under the Jungle

Table 3: Terrestrial cave data requirements

Content	**Format**	**Description**
Line survey	Analog -> Spreadsheet	Measurements recorded with a laser rangefinder and compass
Video footage	MP4	4K and 30fps
Photographs	RAW	Still images to compare to video frames
GCP coordinates	CSV	Calculated based on collected coordinates outside the cave
Control maps	Analog	Map from Central Oklahoma Grotto

3.3. Research Design

Different workflows had to be followed due to the differing natures of terrestrial and aquatic caves. The workflows for this study, underwater cave surveying, and photogrammetry are depicted in Figures 9, 10, and 11, respectively. Once the requirements for the test sites were identified and the software licenses were purchased, each member of the survey teams was briefed on the basic principles of caves and photogrammetric survey. After arriving at the test sites and reviewing the survey methods, coordinates outside the caves were collected where there was as little tree cover as possible. For the terrestrial caves, as the traverse survey was being conducted, targets were placed at the turning points to be used as GCP's. After the final GCP was established, the photogrammetric survey commenced. Photogrammetry can take dozens of hours and multiple attempts depending on how powerful the computer being used is. After the photo alignment, the point cloud, a set of data points in a 3-dimensional space with x, y, and z coordinates attached to each point was refined (see section 3.4.5) before it was optimized. The Gradual Selection tool in PhotoScan offers four methods of selection, which are detailed later in this section. The dense cloud was then built based on the optimized point cloud, and then the final photogrammetry steps of building the mesh and texture were completed. While it is possible to continue without a dense cloud, the dense cloud is a more detailed version of the point cloud that is required for high-resolution models. The points are connected to nearby points to build a mesh, which is essentially the "skin" of a 3D model. The final step of adding texture is what paints a photorealistic image onto the mesh. Once usable models were created, they were imported into ArcGIS Pro to transform the raster data to vector data. The vector data was then used to create the 2D footprint of the photogrammetry model by using its XY extent. This final 2D footprint was then overlaid with previous survey maps for comparison.

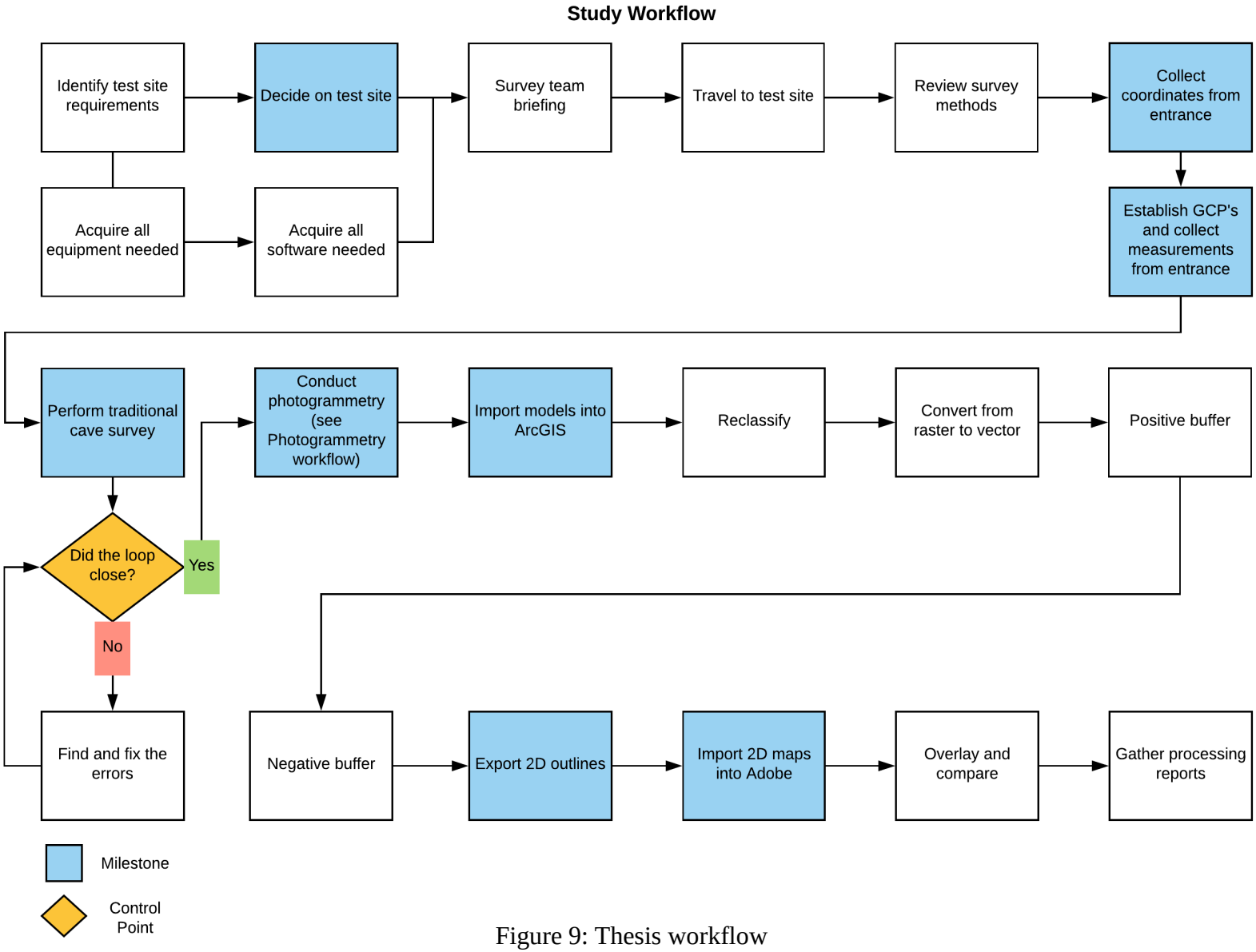

Figure 9: Thesis workflow

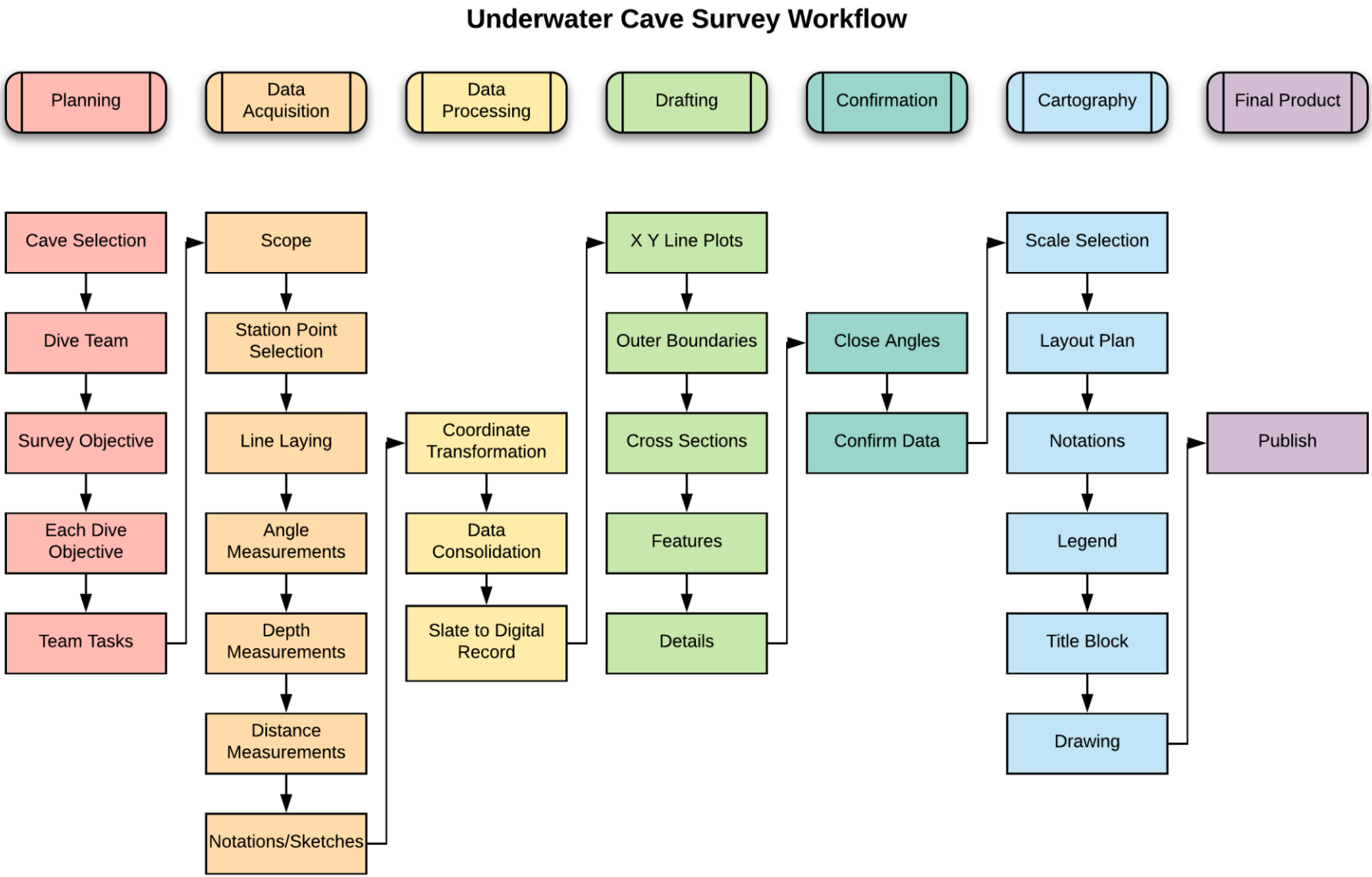

Figure 10: Underwater cave survey workflow

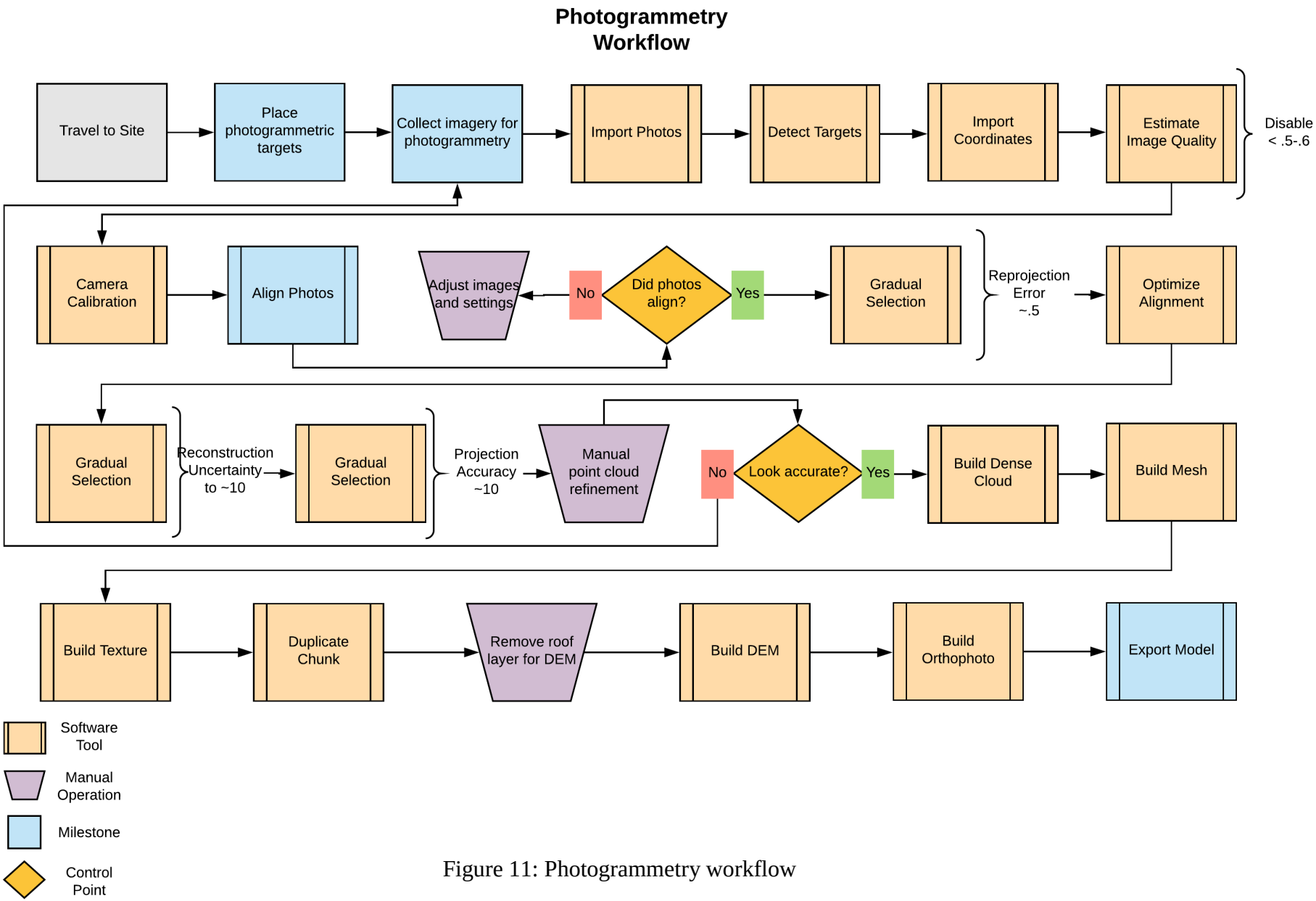

Figure 11: Photogrammetry workflow

The data collection process for the underwater caves was essentially the same as the process for terrestrial caves, with a minor variation due to equipment. A clinometer was not required underwater because a dive computer was used to measure the depth at each survey station. More importantly, with respect to underwater data collection, the camera must remain facing forward, in the direction that the diver is traveling. Additionally, the diver must make sure that other lights do not point in the same direction as the camera and the main floodlight.

The Estimate Image Quality tool, the fourth software tool used in the photogrammetry workflow, is shown in Figure 12. This step removed undesirable images that were blurred from the original data set. An initial visual inspection of the images did not eliminate those that had out-of-focus targets or had blurred edges. Therefore, prior to running the Estimate Image Quality tool and removing the low-quality images, the alignment process in Agisoft did not yield accurate results. A quality threshold of 0.55 was selected for this study, as is recommended to remove images not in focus, and all images that ranked below that number were disabled. Images collected with a better camera would most likely result in a higher mean quality, in which case the user could use a higher quality threshold without inhibiting the alignment process. Removing images below the quality threshold of 0.55 removed roughly 25% of the images. This process is discussed further in Section 3.6.

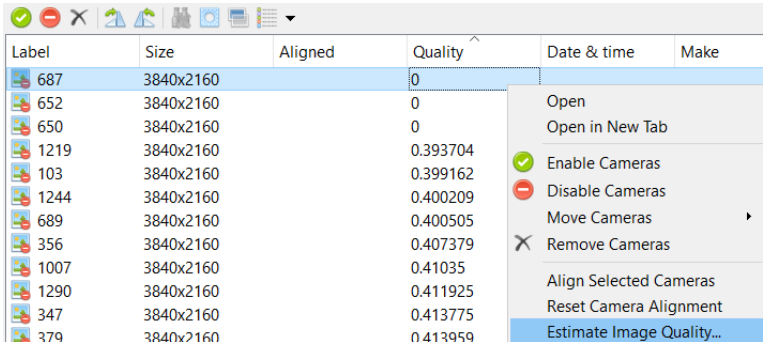

Figure 12: The Estimate Image Quality tool

3.4. Personnel, Equipment, and Software

The goal was to keep this a low-cost method, so price played a key role in the selection of equipment. Nearly everything in this thesis could be upgraded to higher quality with a larger budget. A wide frame lens was required for many of the tight passageways in the terrestrial caves and aquatic cave.

There were several people who helped contribute to this section, and it could not have been completed without them. For the terrestrial cave survey team, Colton Flynn was on point, I was on instruments, Garrett Quinby was on measurements, and Cody Pilgreen was on documentation. In the terrestrial cave photogrammetry, I operated both the camera and light source. For the underwater caves, Christine operated the camera and light source for the photogrammetry.

3.4.1. Scuba Diving Equipment

USC requires that any dive-related research be conducted by students from the American Academy of Underwater Science's (AAUS) scientific diver program. Because there are no organizational members within reasonable distance to provide that training for me, the data collection was contracted to a PADI/TDI cave diving instructor, Christine Loew. Christine has remained in active instructor status for many years and has logged more than 6,000 dives, some of which involved data collection for various other scientific projects.

Special equipment is required to allow humans to travel underwater. Every diver is equipped with a buoyancy control device (BCD), dive computer, air tank, regulator, backup regulator, wetsuit, mask, and fins. For those who are not familiar with scuba diving, the BCD is what the diver inflates with air to adjust buoyancy, a dive computer tracks the amount of air and the depth throughout a dive, and a regulator is the breathing apparatus that connects to the air

tank. There are a few differences with cave diving equipment, particularly the use of a helmet and flashlights and cave divers typically carry three flashlights. To allow more time underwater than traditional air, enriched air nitrox was used for this survey. Nitrox is any nitrogen/oxygen combination with more than the 21% oxygen found in normal air. The use of nitrox reduces the amount of nitrogen absorbed in the tissues by the diver, which allows for more dive time. Any diver using nitrox should be certified in its use and understand its risks and how it works.

3.4.2. Terrestrial Cave Survey Equipment

There are several pieces of equipment required for a cave survey. A laser rangefinder, compass, and survey sheet were used for this study. With four people on the survey team, each member was assigned a task. The person assigned to be on point was who decided where to place the targets for each survey station. The second person read the measurements recorded by the survey equipment. The third person recorded everything onto the survey sheet. The fourth member typically sketches the walls and passages, but that task requires artistic skill and much practice. Because none of team members were experienced sketchers, we decided to have the fourth person write notes and document the process by recording video and photographs. Figure 13 shows the equipment used in the terrestrial cave survey. The survey sheets used in the terrestrial caves can be found in Appendix A.

Figure 13: Equipment used in terrestrial cave survey

3.4.3. Photogrammetry Equipment and software

The image acquisition for photogrammetry only requires a camera and a light source. In this study, I chose to use a Canon 70D DSLR, GoPro Hero 5, and a variable 2,500-lumen floodlight for the terrestrial caves. The underwater caves required a more powerful light source and a 30,000-lumen floodlight was selected. Images collected for photogrammetry needed to have at least 60% overlap to be effective, but using video cut the time needed exponentially by having continuous frames from which to choose. The GoPro was chosen due to its extreme durability and waterproof housing. The software used to process the photographs/video was Agisoft PhotoScan Professional (Vers. 1.4 2018). The processing reports for Ice Cave and Owl Cave are in Appendix B.

3.4.4. Camera Calibration

Lenses come in many different shapes and sizes, each causing its own distortion in the image collected. In particular, fisheye lenses are known for causing extreme distortion to allow for a wider FOV. Distorted imagery can produce distorted photogrammetry models, but calibrating the camera can minimize this effect. Agisoft Lens is the calibration software that is coupled with PhotoScan Professional. The calibration is performed by collecting a series of images of a checkerboard pattern from different angles and the software measures how the squares become distorted in different sections of the images and then provides the parameters to input into the photogrammetry software that will "undistort" the images. Figure 14 shows the checkerboard image captured by the camera and the file generated by calibrating the GoPro Hero 5. This is the "Camera Calibration" step in Figure 11.

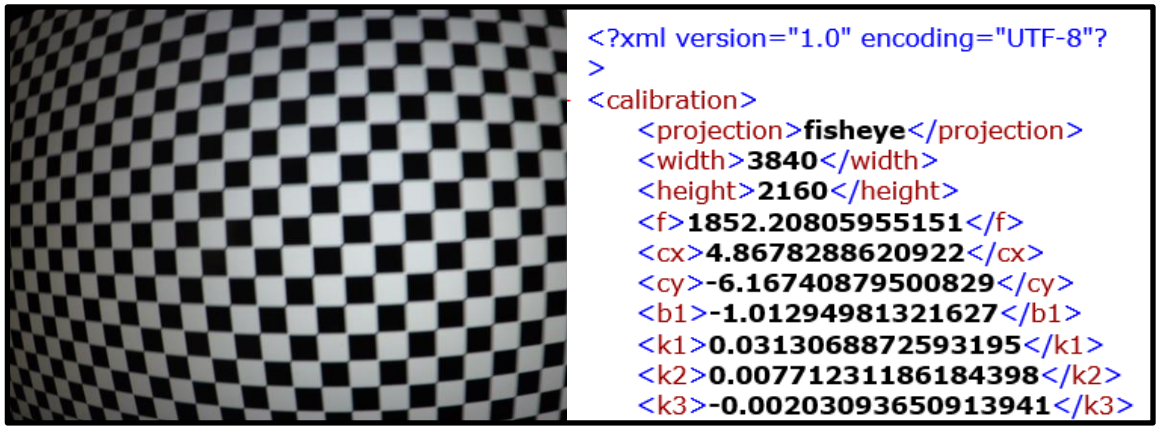

Figure 14: Camera calibration steps

3.4.5. Point Cloud Refinement

PhotoScan's initial attempts at building a point cloud were not as perfect as desired. The Gradual Selection tool within PhotoScan gives the user the ability to select and delete points that do not fall within the user's desired accuracy range. There are four parts to this tool, but only three of them applied to this application of photogrammetry. The first attribute is reprojection

error; this includes false matches and indicates points with poor locational accuracy. Removing points with high reprojection error is the key step in improving point cloud accuracy. The second attribute is reconstruction uncertainty; points with high reconstruction uncertainty noticeably deviate from the object's surface and introduce noise to the model. Removing these points increases the visual quality of the model, but does not increase the accuracy. The third attribute is projection accuracy; this tool filters out points which projections were relatively poor. The final attribute to use to refine a point cloud is image count; the user can require that a point is visible in a specified number of images for it to be used. Image count was not used in this study because simply changing the frame interval will also change how many images each point appears in.

3.5. Target Coordinate Calculations

The two different environments required two different sets of equipment to survey, and thus provided different available measurements. For the terrestrial caves, the instruments provided measurements for GPS coordinates and elevation at the entrance to the cave, and then the target-to-target distance, inclination, and azimuth to each target from the previous target. The GPS coordinates were collected using a Trimble Juno 3B and then imported into Pathfinder Office for differential correction. The original coordinates were at >5m accuracy, but post-processing in Pathfinder increased the accuracy to 2-5m. The base station in Buffalo, which is less than 50 miles from the site, was used for corrections and 100 percent of the 53 points collected were corrected with the base station files. When in underwater environments, a dive computer allows for the depth of each target to be recorded and therefore the z value is determined from that. Without this ability in a terrestrial cave, the elevation of each target must be calculated using simple trigonometry (Figure 15). In this formula, z is elevation, d is target-to-target distance, and α is inclination. It should be noted that a calculator must be set to degrees

instead of radians for this to work correctly. Target coordinates were calculated in Forward3D and ArcGIS Pro. Both software produced the same coordinates in a test run, but ArcGIS was more time consuming for a line survey. The most useful aspect of using ArcGIS Pro was that it showed the points overlaid onto a basemap to verify they were in the correct location. The reason two methods were used was because Forward3D was much faster for a line survey while ArcGIS Pro produced results instantaneously for a radial survey. Details are provided below.

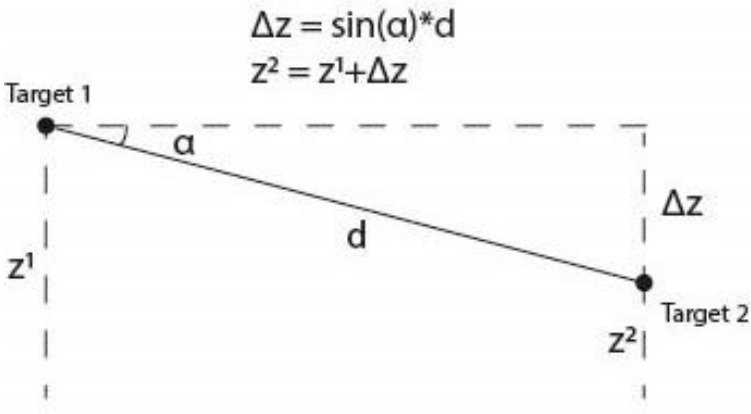

Figure 15: Target elevation calculations

3.5.1. Forward3D

Because this is a 3D space, the x and y coordinates of Target 2 need to be calculated based on the known coordinates of Target 1. Caves tend to be narrow, linear structures so most targets will only have the previous and following targets within a line of sight. For this study, a console application, Forward3D was used to perform these calculations to reduce the probability of human error interfering with the calculations. Note that the elevation of Target 1 must be known before this calculation can be performed. Highlighted in Figure 16 are the measurements input into Forward3D and the output coordinates for one target-to-target pair. This was repeated for each pair of targets. A laser rangefinder was used instead of a tape measure because precise

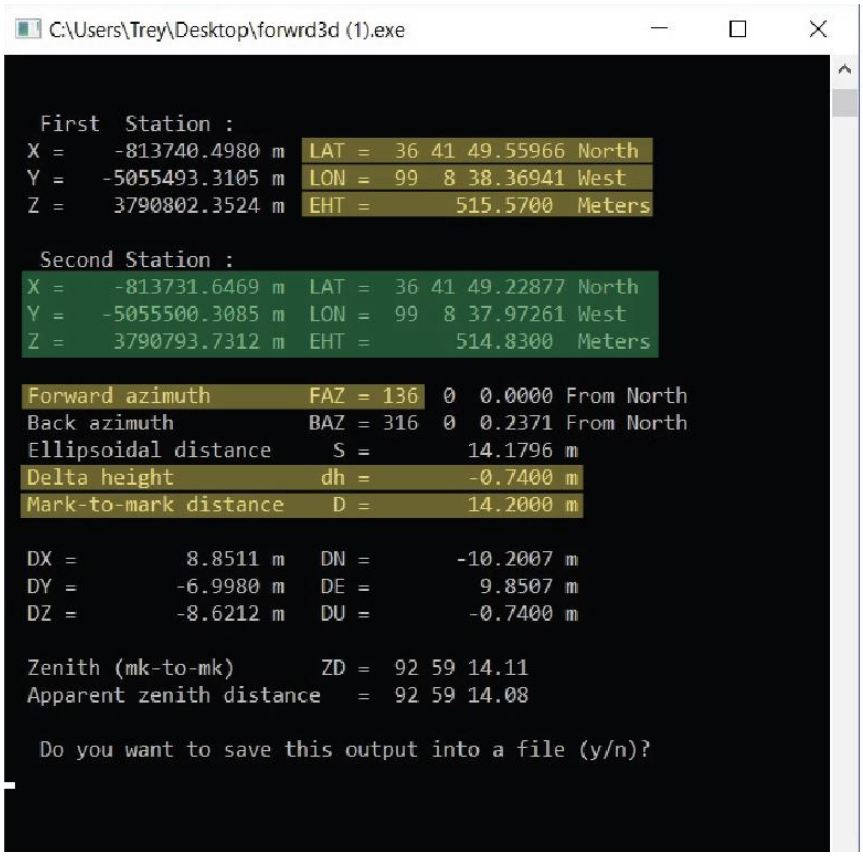

Figure 16: Output file from Forward3D, with input values highlighted in yellow and the output coordinates highlighted in green.

measurements were required for this method, as one bad measurement would reduce the accuracy for every subsequent target after.

3.5.2. ArcGIS Pro

A different method was used for Owl Cave because it was one large main chamber. Using ArcGIS, the starting coordinates were input with their distance to each target like a radial survey. This was performed to show the potential time that can be saved in target coordinate calculations using a GIS in areas with a line of sight to each target. Figure 17 shows the result of using the Bearing Distance to Line, Feature Vertices to Point, and Add XY Coordinates tools within ArcGIS Pro.

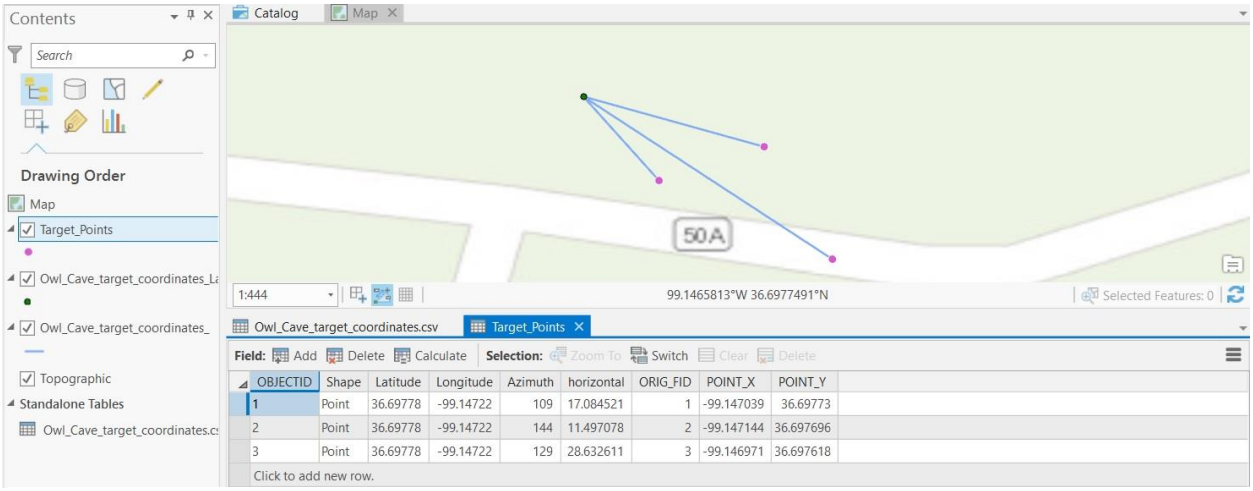

Figure 17: Bearing Distance to Line tool used in ArcGIS Pro

3.5.3. Cave Editor32 and CaveXO

Before photogrammetry and TLS were being used to survey caves, CaveXO was a popular software for cave surveying. The line survey mentioned before would be digitized and input into Cave Editor32 to create a survey table format usable by CaveXO. They surveyor would then have the option to create a line plot of the data or a 3D model based on the LRUD measurements at each station. These models are not georeferenced, but CaveXO could generate a

rough DEM. This study compares a CaveXO survey model with the photogrammetry model to show the advances made in the technology available for cave surveying.

3.6. Data Filtering

Using still frames from video resulted in many less-than-optimal images in the photo alignment. A blurry or black frame prevented sections of images from aligning correctly, especially if pair pre-selection was enabled within Agisoft PhotoScan. Agisoft provides a tool called Estimate Image Quality that can be utilized to sort out less-than-optimal data. The tool assigns a number value between 0 and 1 to each image where 0 is worst and 1 is best. The user can then select all images below a desired value and disable them before the alignment process begins. The reduction in images also reduced processing time.

Extreme precision is required when collecting the measurements during the survey because the traverse data are how the GCP coordinates are calculated. Laser rangefinders are affordable and make distance measurements simple, but tools like total stations that also provide precise compass measurements can be expensive and not always available. When using a compass, even one degree off can lead to an error of several meters, which will then add to any error after that point also. For this project, once a model was built and georeferenced, PhotoScan assigned an error value to each target based on how many meters the target coordinates in the model deviate from the input coordinates. If some of the target coordinates were incorrect, the axis orientation for the model also appeared incorrect. A model only requires at least three active targets for it to be georeferenced, so the accuracy of the model was increased by disabling the targets with the highest error value. Once those targets were disabled, simply clicking the "refresh" button instantly fixed axis orientation issues.

3.7. Data Output

This study produced several different forms of data. The traditional cave surveys produced line maps based on the numbers collected, and the photogrammetry produced various forms of 3D models. Photogrammetry can provide a point cloud, mesh, texture, DEM, and orthophoto. The orthophoto was imported into ArcGIS to create a footprint to be overlaid with an analog map to show the difference in both methods.

Chapter 4 Results

This chapter presents the results of both the terrestrial and underwater cave surveys. The results from Cenote Taj Mahal are presented first and followed by the results for the two terrestrial caves, Ice Cave and Owl Cave. Intermediate outputs from the Agisoft processing are presented along with the final 3D model for each cave.

4.1. Cenote Taj Mahal

The underwater portion of this study proved to be more difficult than anticipated. Despite Christine's best efforts, there were errors in the data collection process that given time and funding constraints could not be corrected with additional data collection dives. Without all the required measurements, I was unable to perform the coordinate calculations accurately for the targets. Approximately half of the Deep Bone Room built inside PhotoScan, but the camera was not operated correctly and sufficient imagery was not captured to build the passage to the chamber. Figure 18 shows the portions of the Deep Bone Room that built correctly as well as the large holes where data was missing that were unable to align.

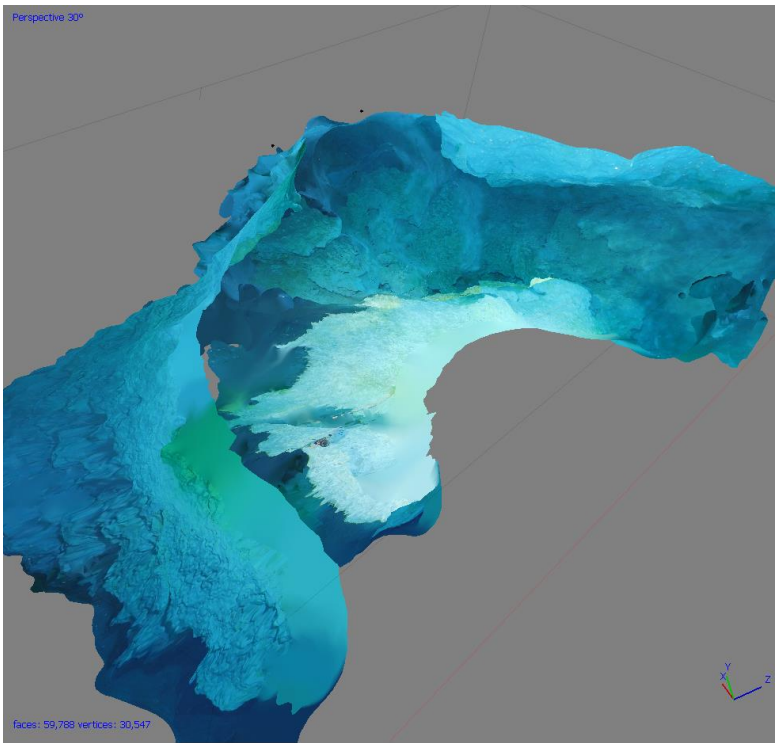

Figure 18: 3D model of the Deep Bone Room

Most underwater caves have survey lines in place with some survey data available from the landowner. It was decided to place the photogrammetry targets along the cave line at each turn. For larger chambers, the targets were placed evenly around the room. It should be noted that the current in the water can move a target, so the targets must be attached securely or weighted down by a dense object.

Unfortunately, the camera was set to record in 1080p instead of the 4K requested, which resulted in a loss in quality of imagery that made the photogrammetry more difficult. The low image quality coupled with the numerous harsh shadows being cast by body parts and equipment resulted in inconsistency between frames. The inconsistency caused the photogrammetry software to be unable to recognize tie points between frames because of the light changes that resulted in different pixel values. Figure 19 shows how much the light changed within a short

distance. This change in pixel value is the primary reason a moving light source is not recommended for photogrammetry. When using a moving light source, it is important to have a much higher overlap percentage than the 60 percent recommended for standard photogrammetry. Pulling still frames from video eases this burden because the user can choose exactly how many frames to pull, whether it be every tenth frame or two frames for every second.

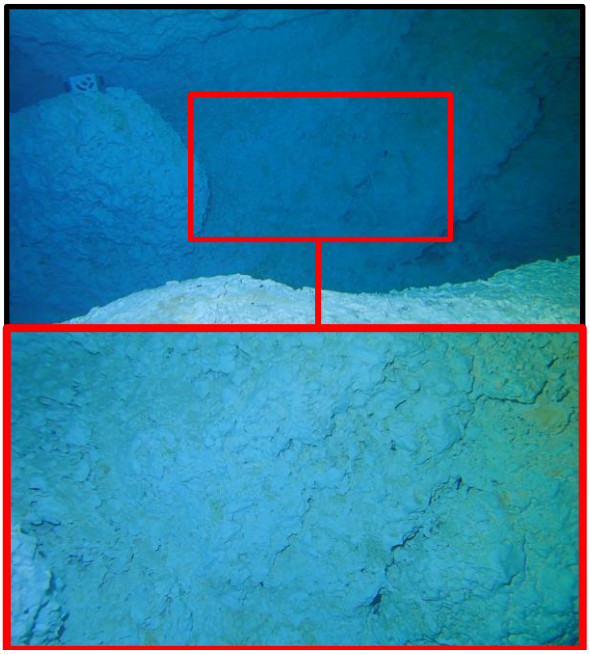

Figure 19: Comparison of two frames showing how much light underwater changes the pixel value over a short distance

Cenote Taj Mahal is large with multiple cave lines and entrances. The Deep Bone Room was chosen as the area of focus because it was away from the tour groups. The visibility was excellent with minimal turbidity upon entry. However, a single trip around the room kicked up the sediment that had settled to the bottom of the cave. The sediment constantly flows through the water, which can cause additional false matches of tie points or even hinder pair selection entirely. Sediment is not a problem that occurs in terrestrial caves, but it means that an underwater cave surveyor will not have the option of multiple attempts in the same dive or possibly even the same day. The video quality on the return trip to the entrance supports this.

Figure 20 shows half of the Deep Bone Room that was built compared to the video from approximately the same position with visible sediment.

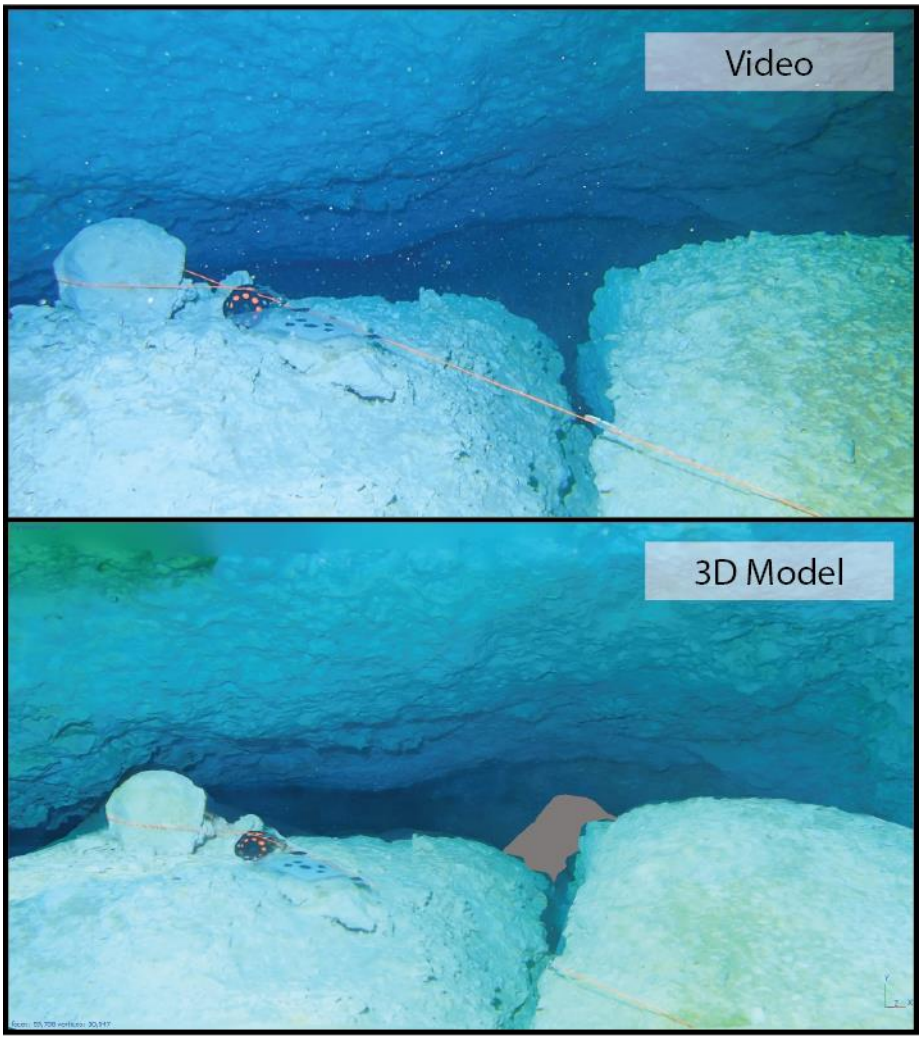

Figure 20: Comparison between the video and the 3D model for the Deep Bone Room

Most of the photogrammetry attempts resulted in an inaccurate point cloud with intersecting planes. This was because of how the camera was positioned and angled throughout the dive. Figure 21 is an example of one such point cloud. If the mesh was built from this point cloud, then it would not look anything like the actual chamber.

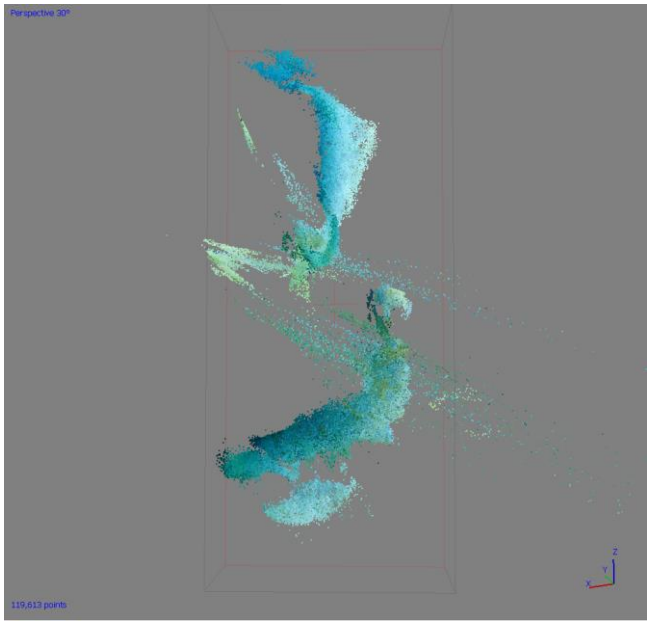

Figure 21: Incorrect point cloud

4.2. Ice Cave

The terrestrial cave survey team started with Ice Cave because of the complex geometry of the walls and because there is a distinct fork in the passages that would be easily comparable to the map from a prior survey. After the first few stations, the survey flow became smooth and consistent as each member became more familiar with his role. The team spent several hours scouting and surveying the cave, and we started the photogrammetry from the entrance after the final target was surveyed. Ice Cave was processed in multiple sub-models, called chunks, because it consisted of more than one passageway. The chunks were aligned and merged at the end of the photogrammetry process.

To show how different the results from 3D surveying can be, I chose to show the models from both the CaveXO and Agisoft PhotoScan. The table in Figure 22 below shows how the measurements from the traditional survey must be input into Cave Editor32 before being exported into CaveXO. Tape is distance, Comp refers to azimuth, Inc is the inclination given in

both negative and positive values accordingly, Up is distance to ceiling, Down is distance to floor, Left is distance to the wall left of the target and Right represents distance to the wall right of the target. This data comes from the “Perform traditional survey” step in Figure 9.

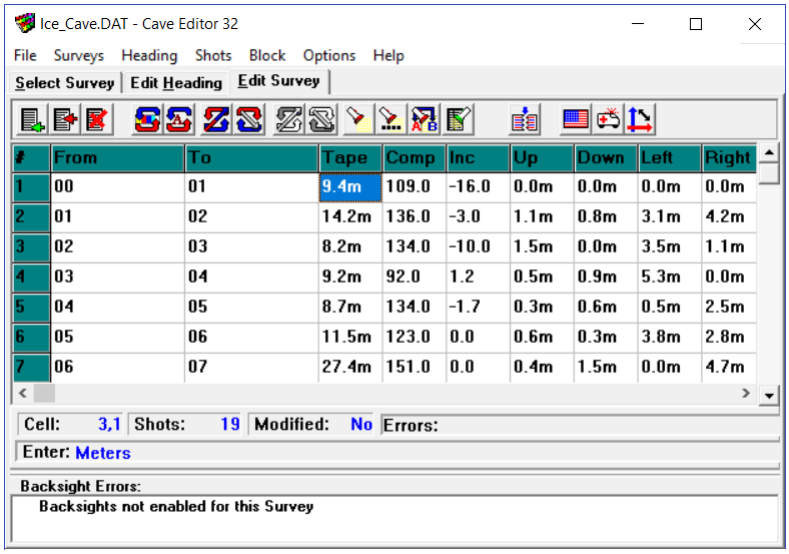

Figure 22: Survey measurements input into Cave Editor32

CaveXO creates a basic line plot of the survey from the input data and then uses the LRUD measurements from each survey station to build a 3D model of the cave. Once built, different settings can be toggled on or off to show the survey line, stations, 3D model, texture, and DEM. Figure 23 is the resultant cave DEM constructed from depth calculations (left) and a line plot model based on survey stations (right). The DEM represents the highest points from sea level in red and the lowest points in blue. The line plot model also provides the names of the survey stations.

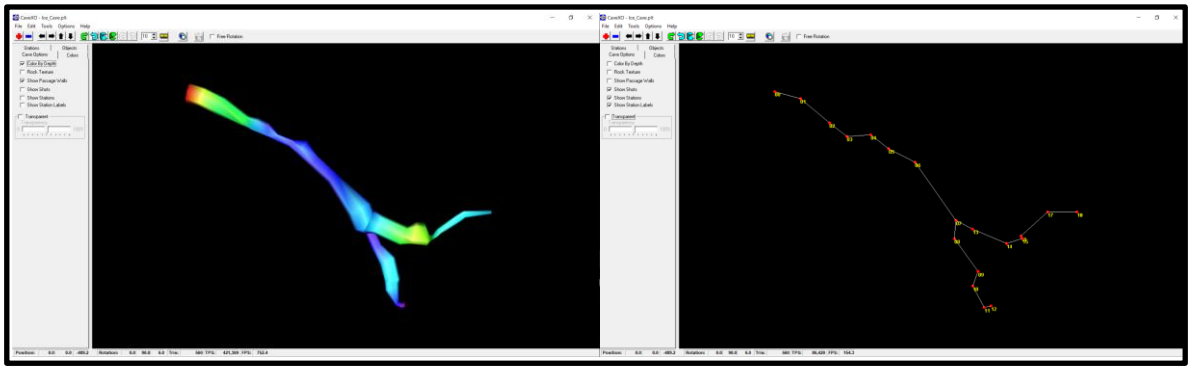

Figure 23: Different views in CaveXO

One of the more notable outputs of utilizing photogrammetry for caves is the DEM, which shows the change in the cave floor's geometry. The DEM from Ice Cave is shown in Figure 24 with a resolution of 9.78mm/pix, where blue hues indicate the lowest points of elevation from sea level in the model and red hues indicate the highest points, similar to the

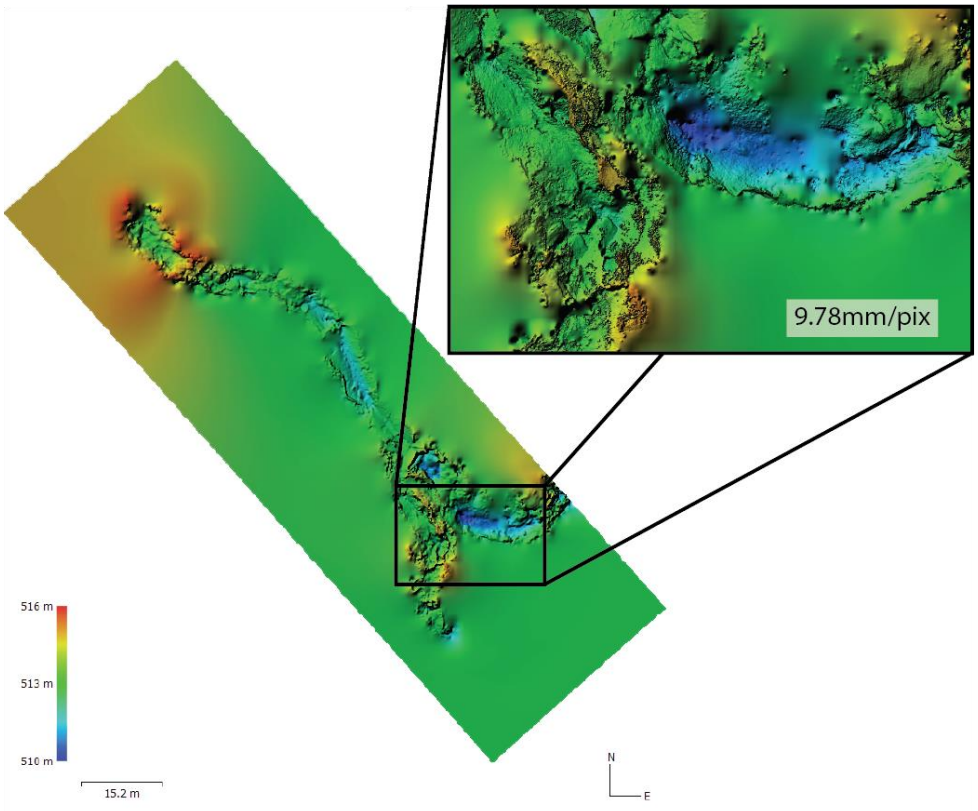

Figure 24: DEM of Ice Cave

CaveXO output. However, the resolution of the DEM from the photogrammetry process is much greater than the DEM from the CaveXO model. This is from the “Build DEM” step in Figure 11.

The DEM will vary in resolution and appearance based on the source data used. Figure 25 shows a side-by-side comparison of DEMs of the same passage built from a sparse cloud, sparse mesh, dense cloud, and dense mesh. The dense cloud takes much longer to generate after the sparse cloud, but it is a necessary cost for a high-resolutions DEM.

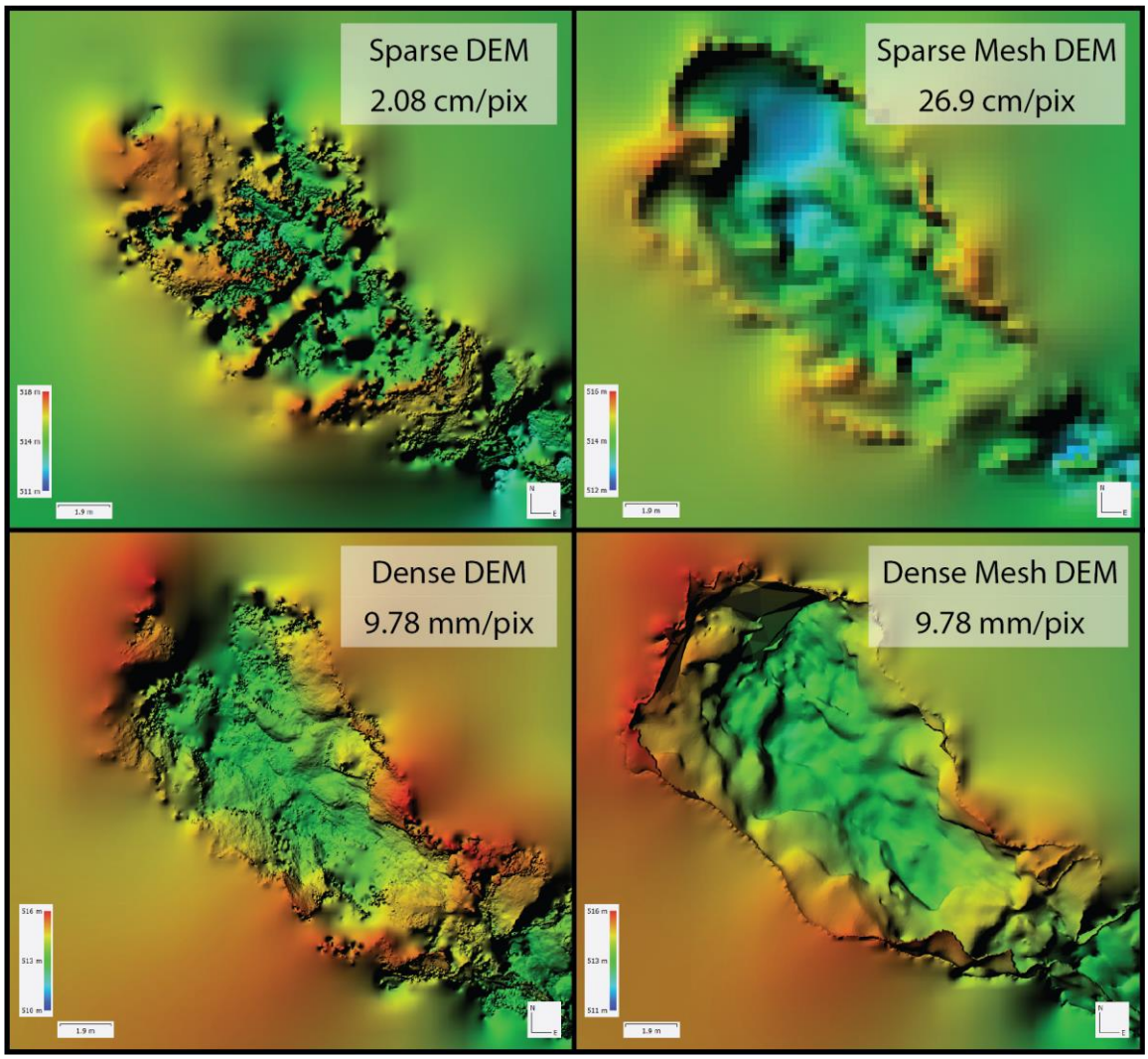

Figure 25: Comparison of DEM's from different source data

The accuracy drawbacks of photogrammetry compared to LiDAR scanning are well known within the 3D modeling community, and the full 3D model of Ice Cave is an example of how much the accuracy can vary from a traditional survey. Figure 26 below shows a comparison of the photogrammetry model to the 1976 survey, and it also highlights areas of obvious differences. This is from the "Overlay and compare" step in Figure 9.

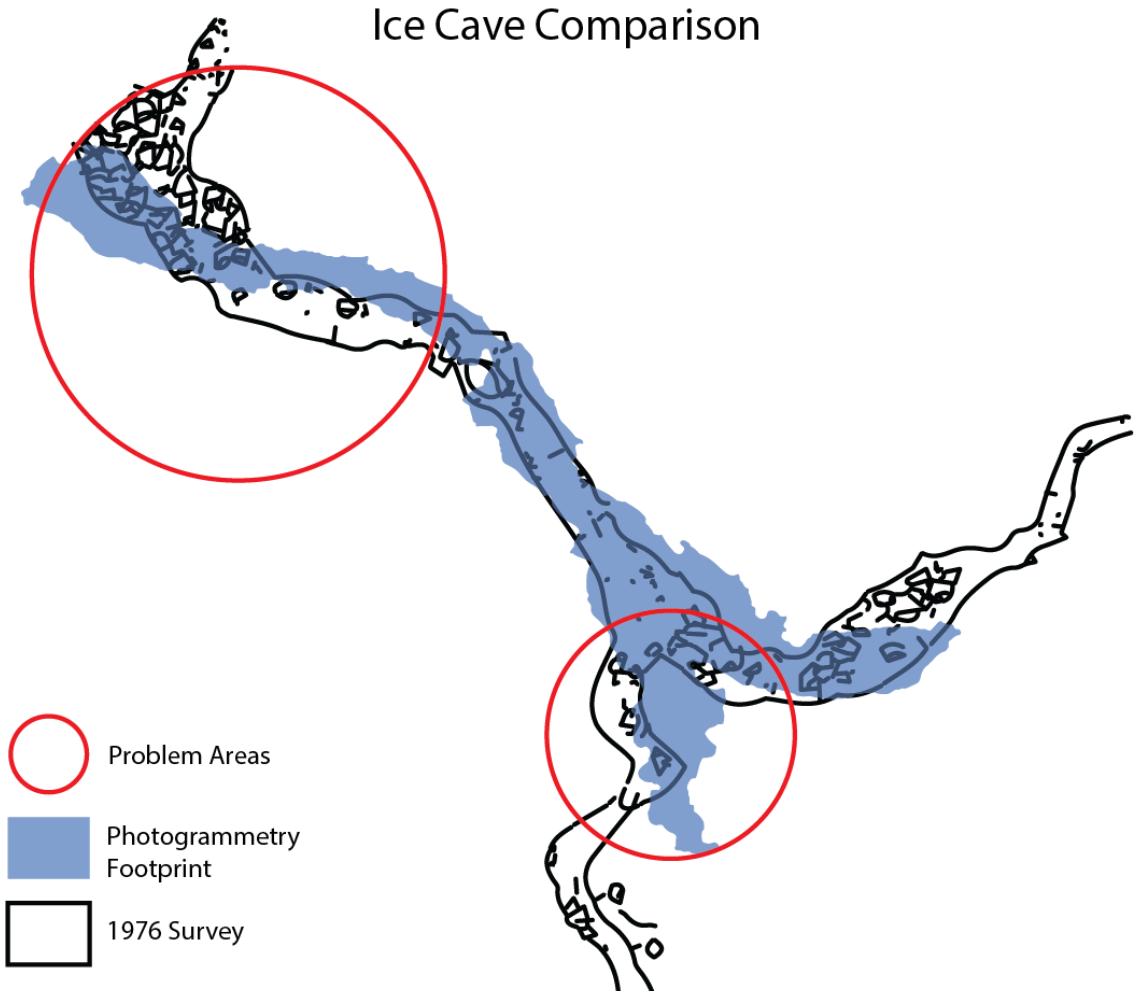

Figure 26: Ice Cave comparison between traditional and photogrammetric surveys

The time difference between the original survey and this one was more than 40 years, but not long enough for a drastic change in the shape of the entire cave. The original survey stations are unknown, but the wall sketches would have been drawn based off the line survey. If there were any mistakes in how the line survey was performed, then that error would extend to the

final map. Figure 27 shows how the line survey for this study compared with both the original survey map (left) and the photogrammetry footprint (right). Initially, the chunk that contained the eastern passage aligned well with the line survey, but the method used to align and merge the chunks together caused that section to alter itself into a slightly different rotation angle. Another notable difference is how the southern passage compares between the surveys. The photogrammetry model aligns closely with the line survey, but it is drastically different from the 1976 survey.

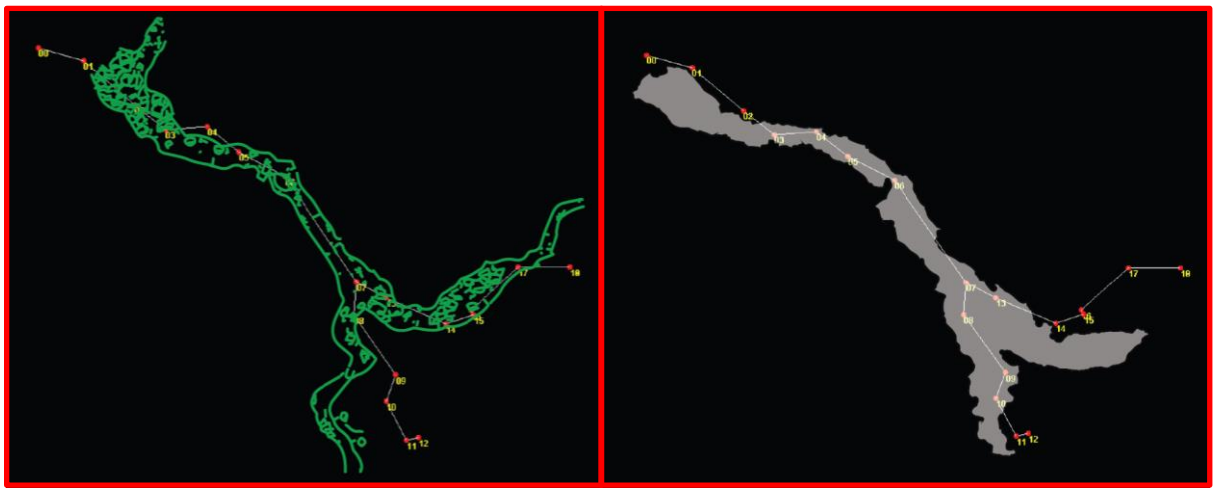

Figure 27: Traverse data compared to traditional survey (left)
and photogrammetric survey (right)

Figure 28 shows the entire georeferenced cave model for Ice Cave as a sparse cloud, dense cloud, and mesh. The textured model was not able to be included here because Agisoft PhotoScan crashed every time the textured model attempted to build. This was likely caused by how the source images were stored within each chunk before they were merged together.

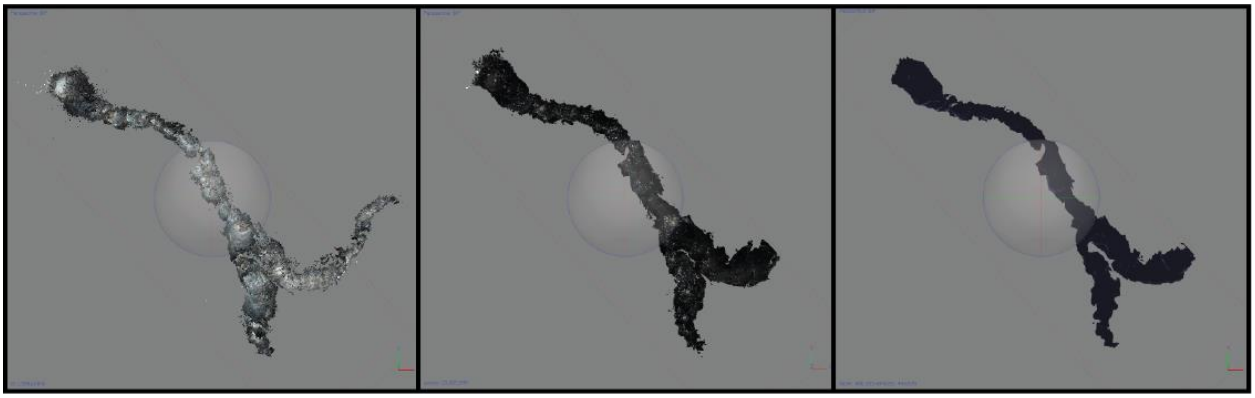

Figure 28: Sparse cloud (left), dense cloud (middle), mesh (right) for Ice Cave

A useful tool in Agisoft PhotoScan is the Measure tool, which allows the user to measure from point A to point B. Figure 29 shows the measure tool used in Ice Cave to determine the extent that the survey team walked to perform the photogrammetry. For the areas of the cave depicted in the 3D model, the measure tool shows that a distance of 175 m was traveled to the final survey station.

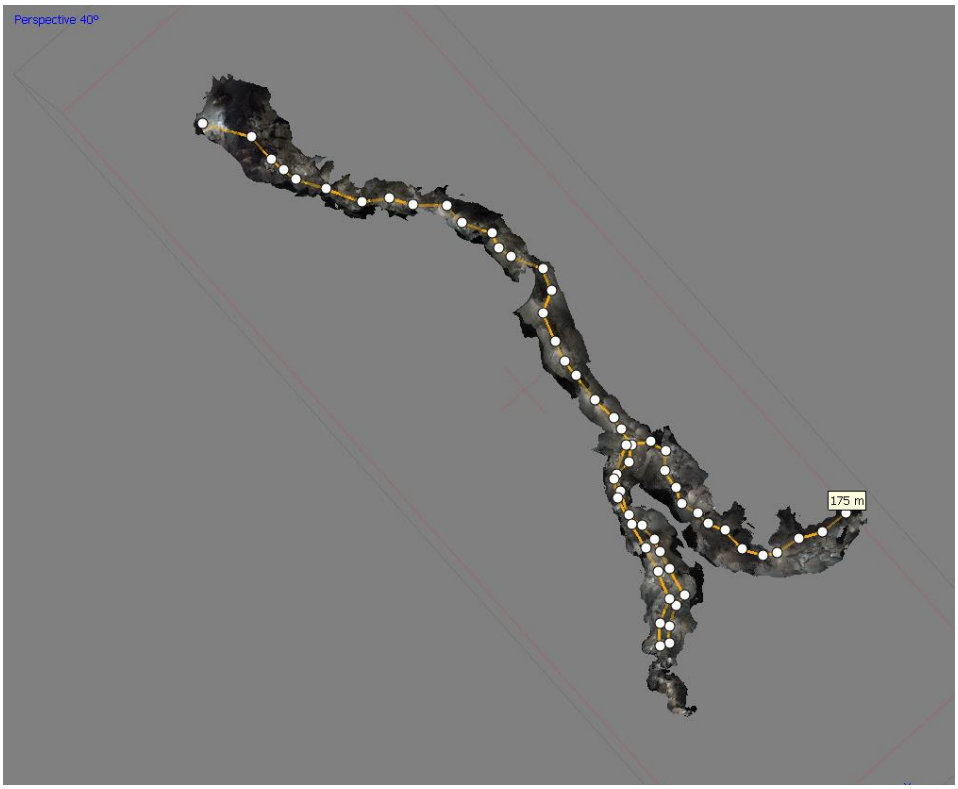

Figure 29: The Measure tool being used in Agisoft PhotoScan

4.3. Owl Cave

Owl Cave consisted of one main chamber followed by a single narrow passage. Targets were placed around the main chamber for a radial survey to save time when collecting measurements. Once the radial survey was finished, the photogrammetric survey commenced. There was only one small passage after the main chamber, so it was not necessary to place as many targets as were needed in Ice Cave.

Figure 30 below shows the photogrammetric footprint (in blue) overlaid onto the original survey map provided by Alabaster State Park. The final turn in the cave was not included in the photogrammetric survey due to flooding and the extremely tight crawlspace to access it. The survey grade for the original map is unknown, but there is a clear indication that the photogrammetric survey produced comparable results to the original survey. It should be noted that the original survey took place between 1976 and 1984, and that changes could have occurred over the years from water erosion and the high amount of human traffic this cave sees each year.

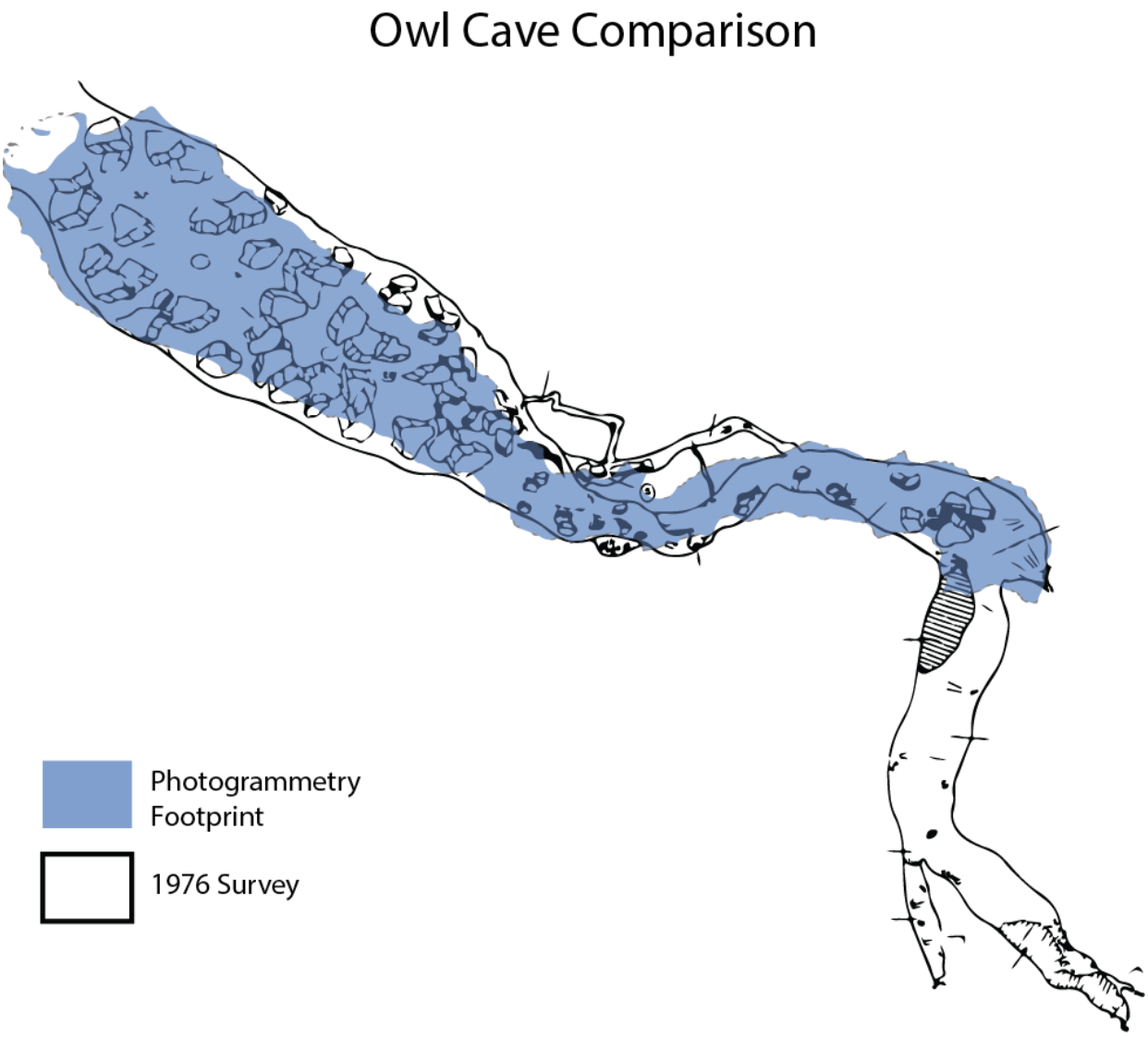

Figure 30: Photogrammetric footprint comparison with traditional survey

The DEM generated for Owl Cave is shown in Figure 31. Highlighted is a tight passage that leads to a direct drop-off into a lower portion of the cave. Due to the heavy rainfall the day before, the entire lower area colored in dark blue was flooded to the point that I could not continue to the end of the cave. Had I not been prepared with the proper equipment, the drop-off could have proved to be too slippery for one person to climb out of alone.

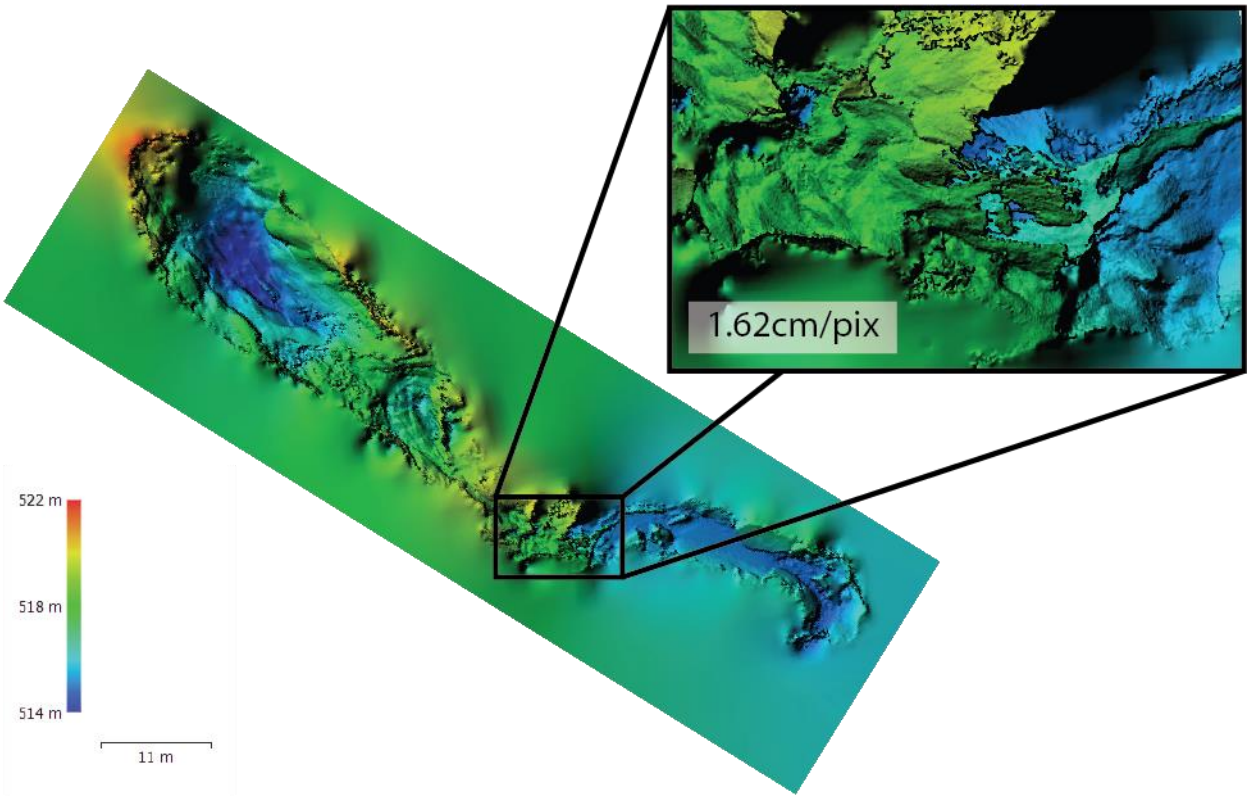

Figure 31: Owl Cave DEM

The photorealism of photogrammetry is what makes it an attractive choice for 3D modeling. Figure 32 shows a comparison of the same cave passage between the video and the tiled model. It should be noted that the fisheye lens used to record the video creates distortion that is corrected in the photogrammetry model. It is also difficult to position the virtual camera in the 3D model to the exact same position in the video frame.

Figure 32: Survey video comparison with tiled 3D model

As mentioned in the Ice Cave section, there is more to a 3D model than the final textured model. Figure 33 shows a close-up view of the point cloud, wireframe, mesh, and textured model. The wireframe is essentially the “skeleton” of the mesh that can be used to determine sections with an insufficient amount of data to build an accurate mesh. Natural features are rarely totally flat, so larger triangles in the wireframe indicate that fewer data points in the point cloud were available.

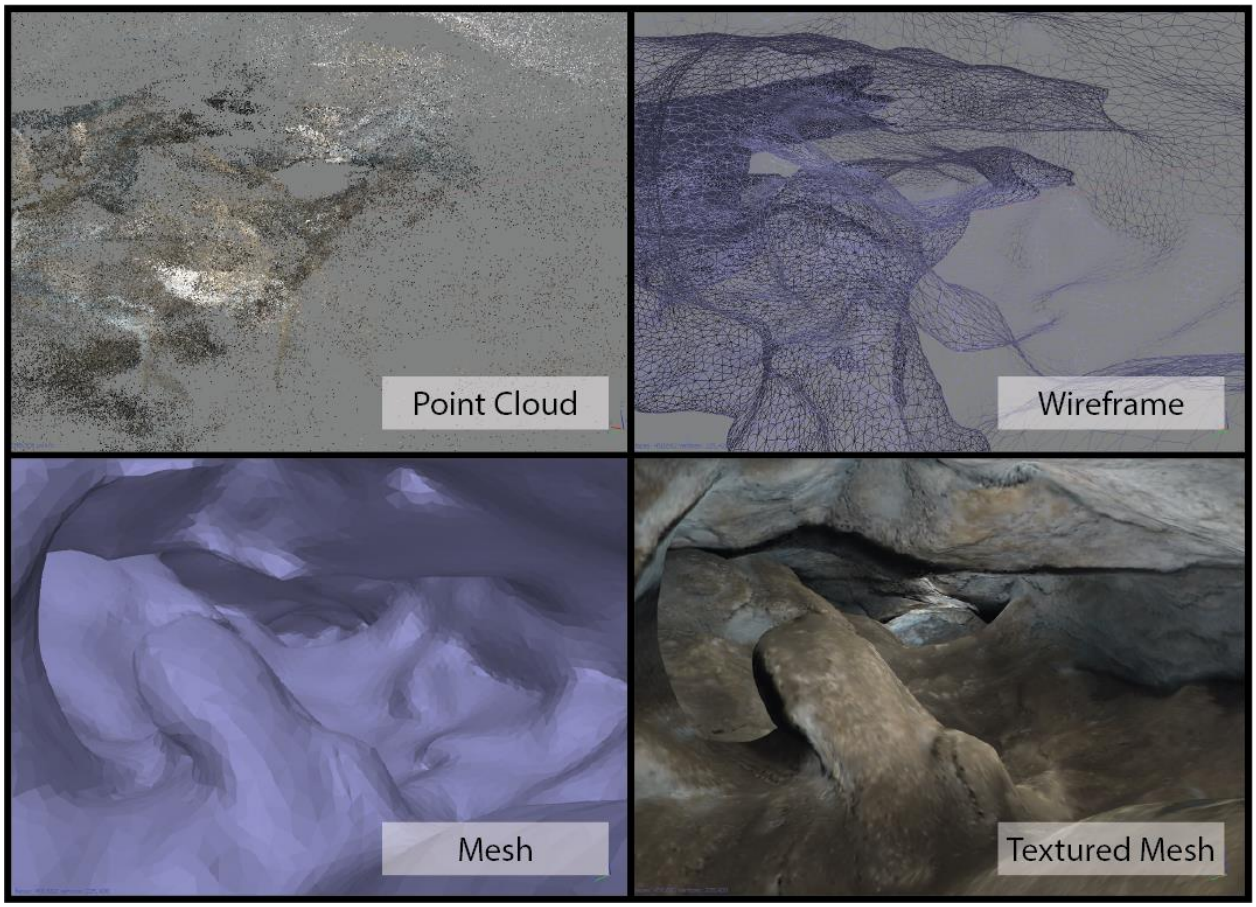

Figure 33: The point cloud (top left), wireframe (top right), mesh (bottom left), and textured mesh (bottom right) for Owl Cave

Chapter 5 Discussion

This study proved to be more difficult than anticipated on all fronts. Some of the obstacles faced were to be expected, while other ones were not predictable at all. Each cave was unique and required on the spot thinking to tackle successfully. As a result, many recommendations are made for future work. The obstacles are discussed in the next section while recommendations are discussed in section 5.4.

5.1. Obstacles Faced

There were obstacles nearly every step of the way during this study. Selecting the sites for the terrestrial caves was easy because the Alabaster Caverns were only a short drive from my home, but the underwater cave selection went through several different caves before Taj Mahal was selected because of how the weather was affecting the area at the time. During the photogrammetry process, there were many times I had to restart a model from the beginning because of either an error I made or a simple optimization step I took too far.

5.1.1. Scouting Locations

Due to how much diver traffic affects the turbidity, the portion of the underwater cave to be surveyed needed to be an area not typically used by tour guides. Having local knowledge of the diving community helped determine a few potential caves that would be sufficient locations. However, there was a tropical storm during the week of the survey that caused most of the ocean divers to have to use cenotes instead. This major increase in diver traffic greatly affected the turbidity in some of the caves and made most of the locations no longer suitable for this study. Thanks to the knowledge provided by Christine, the Deep Bone Room of Cenote Taj-Mahal proved to be a great location with low turbidity on the route to it.

If attempting to use photogrammetry in an underwater cave environment, it is important to have a site where there is not much traffic from divers. Inexperienced divers, or even multiple experienced divers, can stir up sediment in the water with the kicks of their fins. These particles add to the turbidity and can ruin a set of imagery, rendering it unusable. The image in Figure 34 below was pulled from the return trip to the entrance, which shows how badly the kicked-up particles affect the imagery.

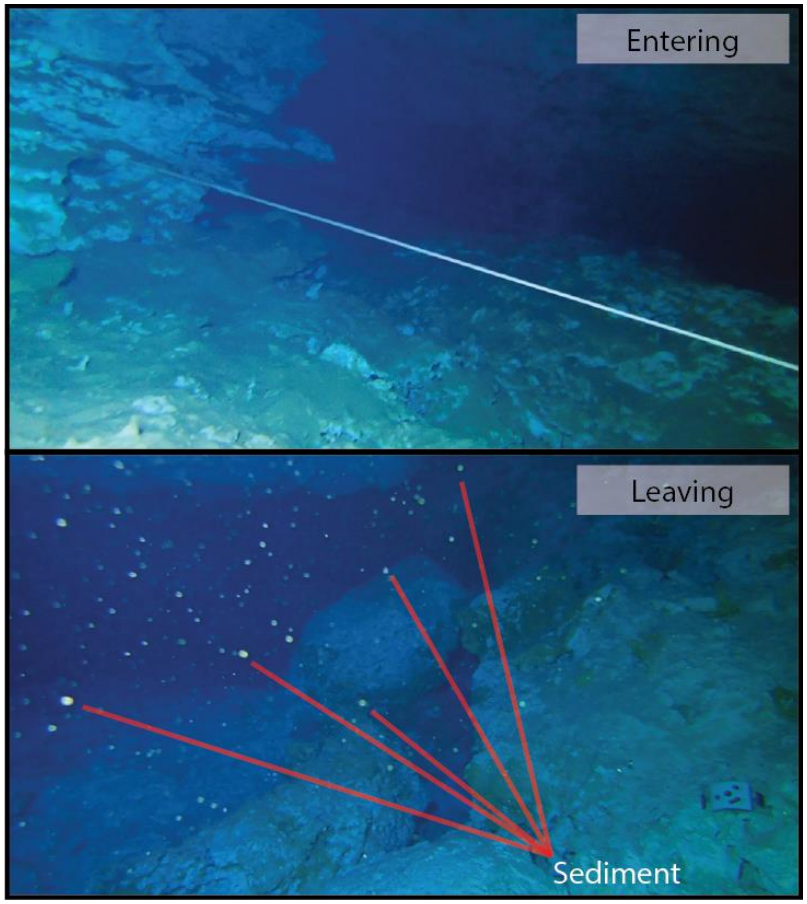

Figure 34: Video entering cenote (top) compared to video exiting cenote (bottom)

5.1.2. Lighting

It was expected that a 2,500-lumen floodlight might not be suitable for all areas of underwater caves, which was proven true after the first dives. It worked great for most of the short and narrow passageways, but some of the larger ones remained relatively dark. Fortunately,

Under the Jungle dive shop had 30,000-lumen floodlights available to rent. This brighter light reached much farther than the 2,500-lumen light, but it was also too bright to be used on objects close to the camera. Long, straight passageways would likely require the more powerful light, especially if the visibility underwater is somewhat poor.

5.1.3. Operator Errors

After viewing the videos from both the underwater and terrestrial caves, there were several lessons learned regarding how to operate the camera. In the terrestrial caves, there were times where the operator may have been moving too fast in some sections. Because the frames are pulled at even intervals, it would have helped to try to remain at one constant slow speed. There were also times where the operator slipped on muddy rocks, which caused a violent shake in the video.

The underwater cave imagery proved that the camera operator must be familiar with both photogrammetry and surveying, despite how skilled a diver one may be. A clear dive plan was provided, but the video shows that there were narrow-beam flashlights other than the floodlight showing up in the camera's FOV. The 2,500-lumen floodlight was chosen because it attaches to the camera to prevent harsh shadows from showing up in the FOV, but it was not attached during the dives and shadows from body parts and equipment were clearly visible. The camera settings were also not set according to the dive plan and much of the video only shows one side of the cave because it was not in wide-angle mode or facing the appropriate direction throughout the survey.

5.1.4. Photogrammetry Issues

There were multiple problems encountered with Agisoft PhotoScan. The first notable bug was during the video import process. The progress bar for the import did not show an estimated

time to be completed and ran for 12 hours before the author decided to cancel and investigate. The computer being used did not have the proper codec installed, and the issue was quickly resolved by finding the correct codec. The second bug with the video import feature was that it would not let the user select portions of the video to import as it is supposed to, but instead would only work if the entire video was selected.

The primary problem of concern with the photogrammetry models was that some of the models displayed correctly while a few displayed with an inverted z-axis. This created a problem with the DEM's from those portions because the color scheme was opposite the correct ones. It was concluded that bad imagery/data were the causes, and the solution was found by decreasing the frame interval and disabling every frame that fell below a 0.44 on image quality along with disabling inaccurate targets as discussed in the next section.

5.2. Error propagation

In environments like caves where high-accuracy GPS units cannot be used to collect GCP coordinates, it is difficult to create perfectly georeferenced models. Depending on how the coordinates are created for the GCP's, they might not match up perfectly to the photogrammetry model. To compensate for that error, Agisoft PhotoScan will shift or rotate the model to where the GCP coordinates have the least amount of variation to the model coordinates. GCPs will each have their own error value (in meters) listed in the reference pane. To increase the accuracy of a model, the GCPs with the highest error values can be disabled so long as at least three GCPs remain active for spatial reference. Target 7 in Ice Cave showed an unusually high error value at 49 meters compared to most of the other targets around one meter. This caused a problem with the axis orientation of the model, but the problem corrected itself once Target 7 was disabled.

5.3. Using Video Instead of Still Photos

There are several benefits to using video instead of shooting still photos for cave photogrammetry, including time and ease-of-use. It also makes it possible to use videos shared online to recreate the environments shown. However, there are also drawbacks with current technology. Consumer-grade cameras can only record video at less than half the resolution of still photos. This lower resolution also provides fewer potential tie points for the software to recognize between frames. If using video in darker environments like caves, a stronger light source may also be needed because the user does not have the option to reduce shutter speed to allow more light into the image.

When modeling single objects or small environments, still photography will produce much greater results and will not require much more time. Current camera technology does allow for video to replace still photography in some scenarios, but it may not always provide optimal results. It is my opinion that caves and aquatic environments are currently the only situations where video should be chosen over still photography for photogrammetry.

5.4. Terrestrial Versus Aquatic Photogrammetry

When comparing the videos from the terrestrial and underwater cave surveys, a few key differences were immediately noticeable. The first was how much darker the underwater caves appeared. Light cannot travel as far underwater, so the more powerful floodlight produced better imagery. A 30,000-lumen floodlight is a great place to start for underwater cave photogrammetry, and a 2,500-lumen floodlight will suffice for most terrestrial cave applications. The second difference was the amount of sediment in the underwater videos. If a mistake is made on the first dive, then it would be best to wait several hours or until the next day to try again.

5.5. Future Research

Neither photogrammetric nor traditional cave surveys can be verified by using satellite/aerial imagery, so one cannot say with certainty which survey is more accurate. The best way to test photogrammetric accuracy would be with the use of a LiDAR scanner. Both point clouds can be georeferenced using the same methods and then the point clouds can be compared. Laser scanning has been established to be the most accurate method of recreating 3D objects in high detail.

It would also be interesting to compare results from different cameras and lens types. Perhaps a slightly narrower (12-15mm) lens could capture all walls with less distortion. GoPro cameras increase in quality with every new model, and the GoPro Hero 7 announced in late 2018 utilizes a new "hypersmooth" electronic stabilization feature. The new feature coupled with a higher capture frame rate in 4K could reduce the number of blurry frames and result in less post-processing time.

Most people choose to use the photogrammetry software they learned with because the workflow for that specific software is what they know. There are numerous other pieces of photogrammetry software out there, each with its own pros and cons. It is possible that something other than Agisoft PhotoScan may produce more accurate cave photogrammetry results, but I have not seen any studies on the subject.

The coordination of the dive team can play a key role in the success of an underwater photogrammetry project. When working in a dive team, the diver who is not holding the camera needs to ensure that he or she does not shine any light into the FOV of the camera. However, they also need to be aware of any shadows that may be caused by their light sources. The diver

holding the camera and light must also make sure that the hoses for the regulators do not drift in front of the light.

For archaeological purposes, photogrammetry is an ideal nondestructive way to recreate artifacts. As long as photos are taken before an artifact is removed from a site, the object can be modeled and then virtually placed in its original location within a 3D model of the site. As technology advances, it would be a good practice to recreate sites continuously like the cenotes because new discoveries are being made every year. If a version of a site is preserved, then new spatial analyses can be performed when a new artifact is found. Archaeology can be destructive sometimes, but photogrammetry allows us the ability to revisit a site to what it was before it was altered. VR can also add to these recreated sites by providing an immersive learning environment for students to interact with objects without the fear of damaging them. Each object can be tied to a database of information about the objects that is accessed when the user interacts with the environment, which provides a visual hands-on approach to a field that is otherwise hands-off to most.

VR also provides the opportunity to train scientific divers, tour guides, and casual visitors. Possible real-world scenarios can be practiced to better prepare a diver for what he or she is about to see. It is common for some divers to experience panic attacks during their first cave dives because it can be such an overwhelming experience and the realization that there is nowhere to surface can take some time to get used to. Cave diving is a dangerous sport, but the use of 3D models can lead to increased safety for recreational and professional divers alike.

5.6. Final Thoughts

Due to the tough constraints required for this study, it was concluded that a data collector should be more knowledgeable and experienced with photogrammetry before attempting such a

difficult task. The methods Jordan (2017) used proved to be an excellent place to start, but there were some minor revisions that needed to be made for this study to be successful. A much stronger light source was needed underwater, and a 1,000-lumen floodlight like the one Jordan used was almost too dim for even some of the terrestrial cave passages. I also used a newer model of the camera he used, which allowed me to shoot in 4K at 30fps. Shooting still photos like in Jordan's study would be too time-consuming in underwater caves, which is why I chose to use video instead of still photos.

I would recommend a few changes to anyone wishing to replicate this study or expand this topic further. The first would be to provide more training to anyone participating who has little experience with photogrammetry. Even the most experienced diver may not produce remarkable results if he or she does not understand the basic principles of photogrammetry. The second recommendation would be to maintain a steady, consistent speed when operating the camera. The faster the movement, the greater the likelihood of blurry frames. A camera that could shoot in 4K for 60 or 120fps could also produce fewer blurry frames. The final recommendation I have is to use the most powerful computers available. The computer used here was comprised of an i7 processor, 24GB RAM, and a GTX 1060 GPU. The upcoming generation of processors and GPU's will decrease the processing time needed for large-scale photogrammetry projects like this one.

References

Auer, Michael, and Alexander Zipf. 2018. "3D WebGIS: From Visualization to Analysis. An Efficient Browser-Based 3D Line-of-Sight Analysis." MDPI. July 21, 2018. Accessed October 05, 2018. http://www.mdpi.com/2220-9964/7/7/279.

BCRA Survey Grades. 2002, November 10. Retrieved from http://bcra.org.uk/surveying/

Bergeon, Yves, Imed Hadda, Vaclav Krivanek, Jean Motsch, and Alexandr Stefek. 2015. "Low Cost 3D Mapping for Indoor Navigation." *International Conference on Military Technologies (ICMT) 2015*. doi:10.1109/miltechs.2015.7153749.

Bhagat, Kaushal Kumar, Wei-kai Liou, and Chun-yen Chang. 2016. "A Cost-Effective Interactive 3D Virtual Reality System Applied to Military Live Firing Training." *Virtual Reality* 20 (2): 127-140. doi:http://dx.doi.org.libproxy1.usc.edu/10.1007/s10055-016-0284-x.

Burge, John W. 1988. *Basic underwater cave surveying*. Branford, FL: The cave diving section of the National Speleological Society.

Canuto, Marcello A., Francisco Estrada-Belli, Thomas G. Garrison, Stephen D. Houston, Mary Jane Acuña, Milan Kováč, Damien Marken, Philippe Nondédéo, Luke Auld-Thomas, Cyril Castanet, David Chatelain, Carlos R. Chiriboga, Tomáš Drápela, Tibor Lieskovský, Alexandre Tokovinine, Antolín Velasquez, Juan C. Fernández-Díaz, and Ramesh Shrestha. 2018. "Ancient Lowland Maya Complexity as Revealed by Airborne Laser Scanning of Northern Guatemala." *Science* 361, no. 6409. doi:10.1126/science.aau0137.

Carlson, Brian M., and Joshua B. Gross. 2018. “Characterization and Comparison of Activity Profiles Exhibited by the Cave and Surface Morphotypes of the Blind Mexican Tetra, Astyanax Mexicanus.” *Comparative Biochemistry and Physiology Part C: Toxicology & Pharmacology*, vol. 208, 2018, pp. 114–129., doi:10.1016/j.cbpc.2017.08.002.

Chase, Arlen F., Diane Chase, John Weishampel, Jason Drake, Ramesh Shrestha, K. Clint Slatton, Jaime Awe, William Carter. 2010. “Airborne LiDAR, archaeology, and the ancient Maya landscape at Caracol, Belize.” *Journal of Archaeological Science*: 387-98.

Cohn, Jeffrey P. 2012. "Bats and White-Nose Syndrome Still a Conundrum." *BioScience* 62, no. 4: 444. doi:10.1525/bio.2012.62.4.19.

"Digitalising a Jumbo 747-8 in 18 Hours 3D Scanning of Plane's Interior." *Industrial Products Finder*, March 23, 2013

Fronczek, Charles J. 1980. “NOAA Technical Memorandum NOS NGS-10: Use of Calibration Base Lines”. National Geodetic Survey. Rockville, Maryland.

Gallay, Michal, Ján Kaňuk, Zdenko Hochmuth, John Meneely, Jaroslav Hofierka, and Vladimír Sedlák. 2015. "Large-Scale and High-Resolution 3-D Cave Mapping by Terrestrial Laser

Scanning: a Case Study of the Domica Cave, Slovakia." *International Journal of Speleology* 44, no. 3: 277-91. doi:10.5038/1827-806x.44.3.6.

Gallay, Michal, Zdenko Hochmuth, Ján Kaňuk, and Jaroslav Hofierka. 2016. "Geomorphometric Analysis of Cave Ceiling Channels Mapped with 3-D Terrestrial Laser Scanning." *Hydrology and Earth System Sciences* 20 (5): 1827-1849. doi:http://dx.doi.org.libproxy2.usc.edu/10.5194/hess-20-1827-2016.

Gonzalez, Arturo H., Alejandro Terrazas, Wolfgang Stinnesbeck, Martha E. Benavente, Jeronimo Avilez, Carmen Rojas, Jose Manuel Padilla, Adriana Velasquez, Eugenio Acevez, and Eberhard Frey. 2014. "The First Human Settlers on the Yucatan Peninsula: Evidence from Drowned Caves in the State of Quintana Roo (South Mexico)." 323-37.

Griggs, Anne, M. Kevin Keel, Kevin Castle, and David Wong. (2012). Enhanced Surveillance for White-Nose Syndrome in Bats. *Emerging Infectious Diseases*, *18*(3), 530–532. http://doi.org.libproxy1.usc.edu/10.3201/eid1803.111751

Holenstein, Claude, Robert Zlot, and Michael Bosse. 2011. "Watertight Surface Reconstruction of Caves From 3D Laser Data." *2011 IEEE/RSJ International Conference on Intelligent Robots and Systems*. doi:10.1109/iros.2011.6095145.

Hunt, Christopher, I. Brooks, G. Coles, and Ryan Jenkinson. 1987. "Archaeological Surveying in Caves." *Cave Science: Transactions of the British Cave Research Association*, no. 14: 83-84.

Jordan, Joseph. 2017. "Modeling Ozark Caves with Structure-from-Motion Photogrammetry: An Assessment of Stand-Alone Photogrammetry for 3-Dimensional Cave Survey." Master's thesis, University of Arkansas.

Koska, Bronislav, and Tomas Křemen. 2013. "The Combination of Laser Scanning and Structure from Motion Technology for Creation of Accurate Exterior and Interior Orthophotos of St. Nicholas Baroque Church." *ISPRS - International Archives of the Photogrammetry, Remote Sensing and Spatial Information Sciences* XL-5/W1: 133-38. doi:10.5194/isprsarchives-xl-5-w1-133-2013

Lee, Trey O., and Simon Manning. "Bevel and 3D Models." 8 Aug. 2018.

López, Luis Alberto Martos. 2008. "Underwater Archaeological Exploration of the Maya *Cenotes*." Museum International, 60: 100–110. doi:10.1111/j.1468-0033.2008.00670.x.

Majid, Z., M. F.M. Ariff, K. M. Idris, A. R. Yusoff, A. Aspuri, M. A. Abbas, K. Zainuddin, A. R.A. Ghani, A. A. Bin Saeman. 2017. "Three-Dimensional Mapping of Ancient Cave Paintings Using Close-Range Photogrammetry and Terrestrial Laser Scanning Technologies." *ISPRS - International Archives of the Photogrammetry, Remote Sensing and Spatial Information Sciences*, XLII-2/W3, pp. 453–457., doi:10.5194/isprs-archives-xlii-2-w3-453-2017.

Matthews, Neffra A. 2008. “Aerial and Close-Range Photogrammetric Technology: Providing Resource documentation, Interpretation, and Preservation.” Technical Note 428. U.S Department of Interior, Bureau of Land Management, National Operations Center, Colorado.

Panaram, Kanchana, and Richard Borowsky. 2005. "Gene Flow and Genetic Variability in Cave and Surface Populations of the Mexican Tetra, Astyanax mexicanus (Teleostei: Characidae)." *Copeia* 2005, no. 2: 409-16. doi:10.1643/cg-04-068r1.

Quintana Roo Speleological Survey. http://caves.org/project/qrss/qrss.htm (accessed February 1, 2018).

Santos, Daniel R. Dos, Aluir P. Dal Poz, and Kourosh Khoshelham. 2013."Indirect Georeferencing of Terrestrial Laser Scanning Data using Control Lines." *The Photogrammetric Record* 28, no. 143: 276-92. doi:10.1111/phor.12027.

Spring, Joe. 2012. "Exploring Caving Accidents, Deaths, and Rescues in the United States." Outside Online. September 13, 2012. Accessed October 7, 2018. https://www.outsideonline.com/1903801/exploring-caving-accidents-deaths-and-rescues-united-states

Stella-Watts, Alejandro C., Christopher P. Holstege, Jae K. Lee, and Nathan P. Charlton. 2012. "The Epidemiology of Caving Injuries in the United States." *Wilderness & Environmental Medicine* 23, no. 3: 215-22. doi:10.1016/j.wem.2012.03.004.

Turner, Eric Lee. 2015. "3D Modeling of Interior Building Environments and Objects from Noisy Sensor Suites." University of California Berkeley.

White-Nose Syndrome. Accessed July 28, 2018. https://www.whitenosesyndrome.org/.

Wycisk, Alicja Maria. 2016. “Use of 3D Models Obtained With Photogrammetric Methods in an Industrial Mineral Mine.” Master’s thesis, Norwegian University of Science and Technology.

Xiong, Xuehan, Antonio Adan, Burcu Akinci, and Daniel Huber. 2013. “Automatic Creation of Semantically Rich 3D Building Models from Laser Scanner Data.” *Automation in Construction* 31: 325–37.

Appendix A

Cave Survey Sheet Cave: Ice Sheet #: 1/1 Date: 7/7/18

Survey Team: Trey Lee, Cody Dilgreen, Colton Flynn, Garrett Quinby

Comments:

Station #: 36° 41' 49.65472" N 99° 08' 38.71223" W 5m accuracy @ 68% confidence

From	To	Distance	Azimuth	Clino	Up	Down	Left	Right	Flag	Comment
00	01	9.4	109	-16						Target 1
01	02	14.242	136	-3	1.1	0.8	3.1	4.2		Target 2
02	03	8.2	134	-10	1.5	0.0	3.5	1.1	3	
03	04	9.2	92	1.2	0.5	0.9	5.3	0.0	4	
04	05	8.7	134	-1.7	0.3	0.6	0.5	2.5	5	
05	06	11.5	123	0.0	0.6	0.3	3.8	2.8	6	6 Replaced with 20
06	07	27.4	151	0.0	0.4	1.5	0.0	4.7	7	Fork @ 7 target and flag
07	08	7.2	190	-4.0	1.5	1.0	4.2	5.7	8	
08	09	~~7.8~~ 15.4	150	5.2	0.5	1.0	3.0	1.1	9	
09	10	6.0	206	-1.0	1.2	2.0	4.5	2.1	10	
10	11	9.7	158	-5.8	0.8	0.9	4.5	1.2	11	
11	12	3.1	91	-24.0	0.5	0.0	1.5	0.5	12	
12	—	—	—	—	0.3	0.3	2.2	1.5		
07	13	7.5	123	2.0	—	—	—	—	13	left @ fork
13	14	14.1	119	-1.6	0.7	0.0	4.1	3.7	14	
14	15	6.4	79	-5.8	1.6	1.1	7.3	1.6	15	
15	16	1.14	343	-30.0	1.0	0.7	2.5	0.0	16	
16	17	13.8	54	-0.5	1.1	0.5	1.5	1.0	17	
17	18	11.4	96	-0.9	0.7	~~0.0~~ 0.3	0.4	2.6	18	
18					0.7	0.0	0.7	0.8		

Cave Survey Sheet Cave: Owl Sheet #: 1/1 Date: 7/8/18

Survey Team: Tracy Lee

Comments:

Station #: 28 @ 36°41'52" N 99°8'50" W 1710ft elevation

From	To	Distance	Azimuth	Clino	Up	Down	Left	Right	Flag	Comment
28	21	18.3m	109	-21	3.5	0	10.5	3.2		
28	22	12.4	144	-22	7.3	1.3	4	1.2		
28	23	28.9m	109	-78	4.7	0.5	7	3.3		

Appendix B

Ice Cave

Processing Report
11 October 2018

Survey Data

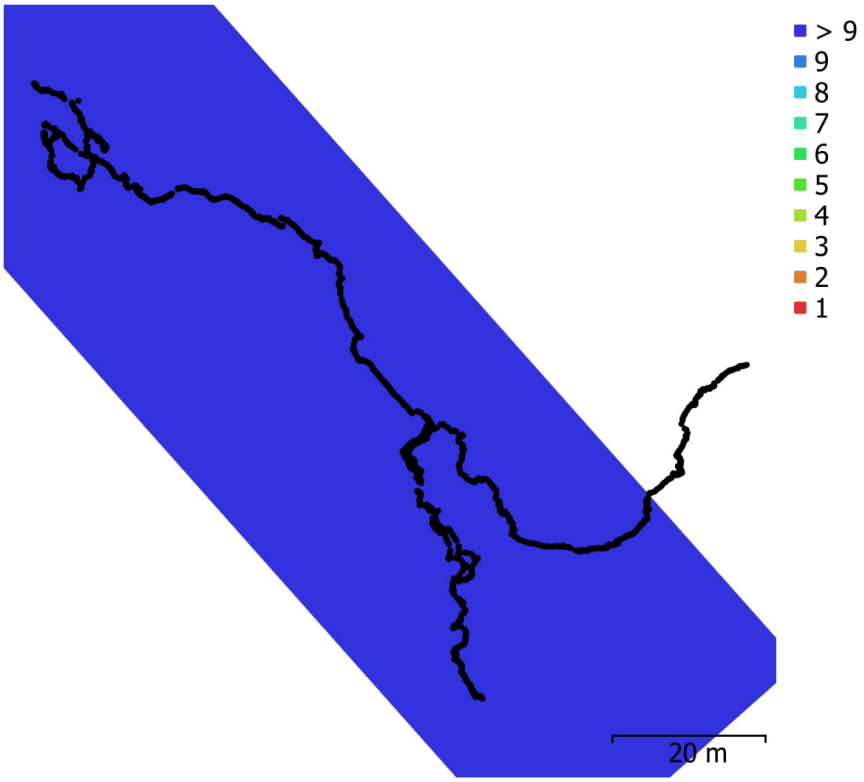

Fig. 1. Camera locations and image overlap.

Number of images:	4,678	Camera stations:	2,750
Flying altitude:	2.55 m	Tie points:	811,588
Ground resolution:	1.22 mm/pix	Projections:	2,184,172
Coverage area:	5.09e+03 m²	Reprojection error:	1.03 pix

Camera Model	Resolution	Focal Length	Pixel Size	Precalibrated
Camera	3840 x 2160	3 mm	3.84e+06 x 2.16e+06 µm	Yes
Camera	3840 x 2160	3 mm	3.84e+06 x 2.16e+06 µm	Yes
Camera	3840 x 2160	14 mm	unknown	No

Table 1. Cameras.

Camera Calibration

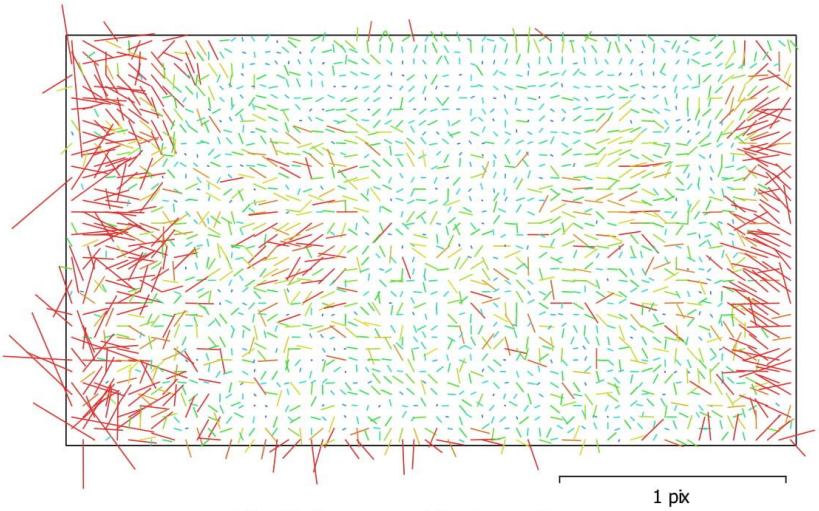

Fig. 2. Image residuals for Camera.

Camera

2143 images, rolling shutter, precalibrated

Type	Resolution	Focal Length	Pixel Size
Fisheye	**3840 x 2160**	**3 mm**	**3.84e+06 x 2.16e+06 µm**

F:	1852.21		
Cx:	4.86783	B1:	-1.01295
Cy:	-6.16741	B2:	0
K1:	0.0313069	P1:	0
K2:	0.00771231	P2:	0
K3:	-0.00203094	P3:	0
K4:	0	P4:	0

Camera Calibration

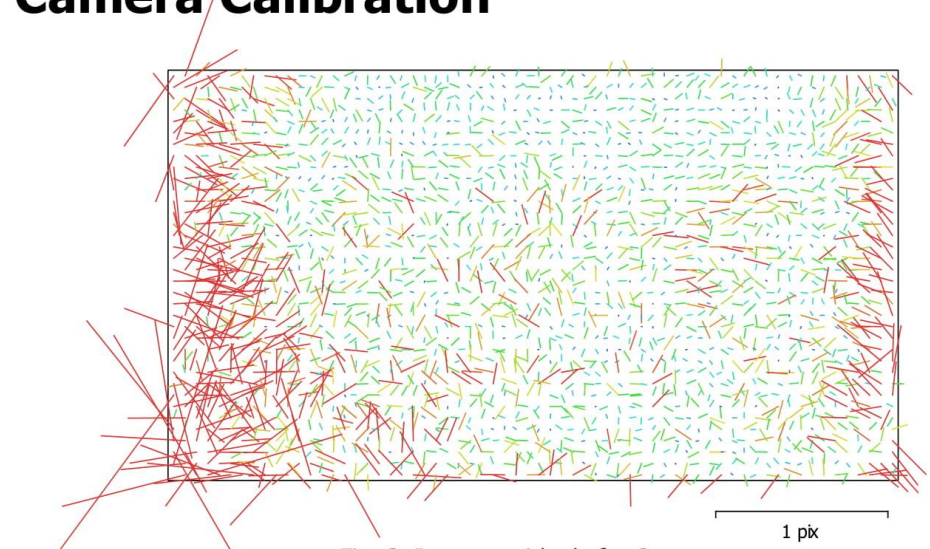

Fig. 3. Image residuals for Camera.

Camera

1899 images, rolling shutter, precalibrated

Type	Resolution	Focal Length	Pixel Size
Fisheye	**3840 x 2160**	**3 mm**	**3.84e+06 x 2.16e+06 µm**

F:	1852.21		
Cx:	4.86783	B1:	-1.01295
Cy:	-6.16741	B2:	0
K1:	0.0313069	P1:	0
K2:	0.00771231	P2:	0
K3:	-0.00203094	P3:	0
K4:	0	P4:	0

Camera Calibration

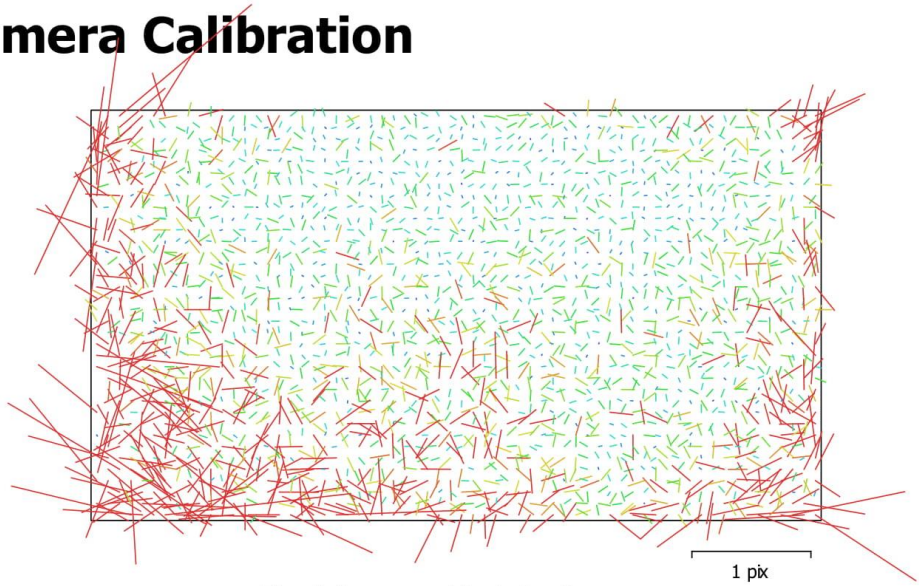

Fig. 4. Image residuals for Camera.

Camera

636 images

Type	Resolution	Focal Length	Pixel Size
Fisheye	**3840 x 2160**	**14 mm**	**unknown**

	Value	Error	F	Cx	Cy	B1	B2	K1	K2	P1	P2
F	**1759.91**	0.2	1.00	0.04	0.09	-0.40	0.03	-0.12	0.15	0.03	0.06
Cx	**10.3037**	0.32		1.00	0.02	-0.00	0.20	0.03	-0.03	0.00	0.03
Cy	**-5.87392**	0.35			1.00	-0.11	-0.01	-0.09	0.05	0.02	-0.29
B1	**-0.563896**	0.11				1.00	0.00	-0.03	0.02	-0.02	-0.06
B2	**-0.98393**	0.096					1.00	-0.03	0.03	0.10	-0.01
K1	**0.053238**	8.4e-05						1.00	-0.91	-0.05	0.16
K2	**0.00526747**	6.3e-05							1.00	0.03	-0.07
P1	**-7.34282e-05**	1.4e-05								1.00	-0.04
P2	**0.000116996**	1.8e-05									1.00

Table 2. Calibration coefficients and correlation matrix.

Ground Control Points

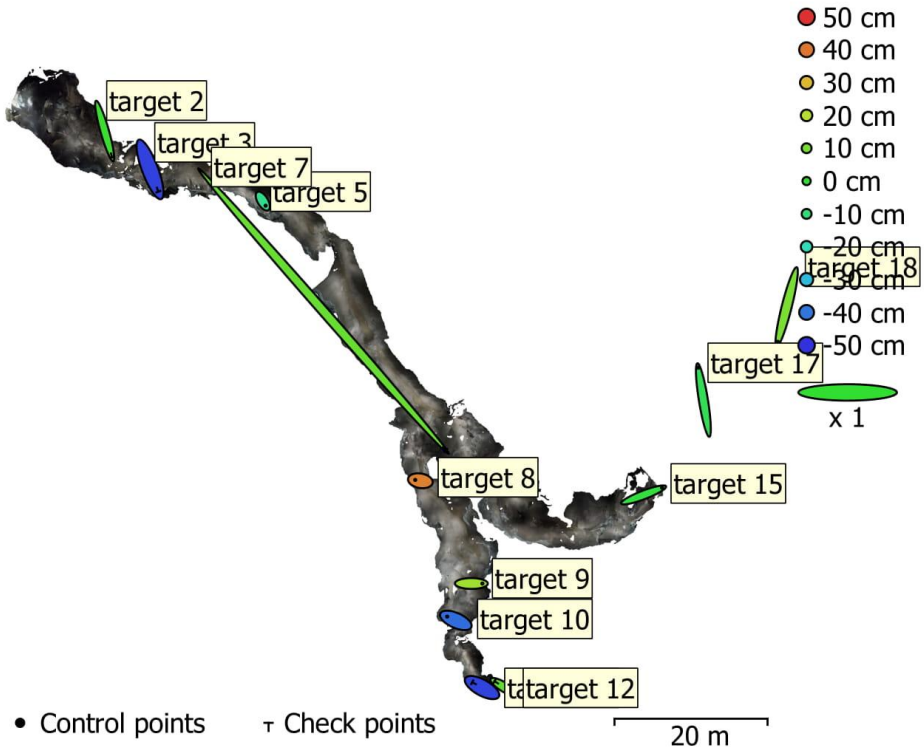

Fig. 5. GCP locations and error estimates.
Z error is represented by ellipse color. X,Y errors are represented by ellipse shape.
Estimated GCP locations are marked with a dot or crossing.

Count	X error (m)	Y error (m)	Z error (m)	XY error (m)	Total (m)
7	2.56902	4.79467	0.232114	5.43955	5.4445

Table 3. Control points RMSE.
X - Longitude, Y - Latitude, Z - Altitude.

Count	X error (m)	Y error (m)	Z error (m)	XY error (m)	Total (m)
5	14.4399	16.8043	0.304173	22.1562	22.1583

Table 4. Check points RMSE.
X - Longitude, Y - Latitude, Z - Altitude.

Label	X error (m)	Y error (m)	Z error (m)	Total (m)	Image (pix)
target 5	0.734861	-1.21038	-0.130419	1.42199	0.105 (32)
target 8	-1.34098	0.224215	0.384998	1.41306	0.059 (22)
target 9	2.87951	-0.0103836	0.160873	2.88401	0.068 (29)
target 10	-2.26113	0.995381	-0.41459	2.50507	0.152 (35)
target 15	4.82475	1.84893	-0.0219213	5.16693	0.039 (7)
target 17	-1.36601	8.4581	-0.0499267	8.56785	0.056 (7)
target 18	-2.30486	-9.13552	0.105685	9.42238	0.003 (14)
Total	**2.56902**	**4.79467**	**0.232114**	**5.4445**	**0.098**

Table 5. Control points.
X - Longitude, Y - Latitude, Z - Altitude.

Label	X error (m)	Y error (m)	Z error (m)	Total (m)	Image (pix)
target 2	1.94807	-6.86644	0.0144257	7.13745	0.049 (30)
target 3	2.18468	-5.80515	-0.4771	6.22095	0.077 (47)
target 7	31.9551	-36.4251	0.0790012	48.4554	299.393 (24)
target 11	-2.56261	1.40244	-0.473273	2.95936	0.095 (19)
target 12	-2.50793	1.52535	0.0674184	2.93614	0.292 (9)
Total	**14.4399**	**16.8043**	**0.304173**	**22.1583**	**129.137**

Table 6. Check points.
X - Longitude, Y - Latitude, Z - Altitude.

Scale Bars

Label	Distance (m)	Error (m)
target 2_target 3	7.76818	-0.431821
target 7_target 8	5.55023	-1.64977
target 7_target 8	5.55023	-1.64977
target 8_target 9	16.1898	0.789767
target 9_target 10	6.35064	0.350641
target 10_target 11	9.244	-0.456004
target 11_target 12	3.00454	-0.0954587
target 17_target 18	10.9468	-0.453238
Total		**0.921895**

Table 7. Control scale bars.

Digital Elevation Model

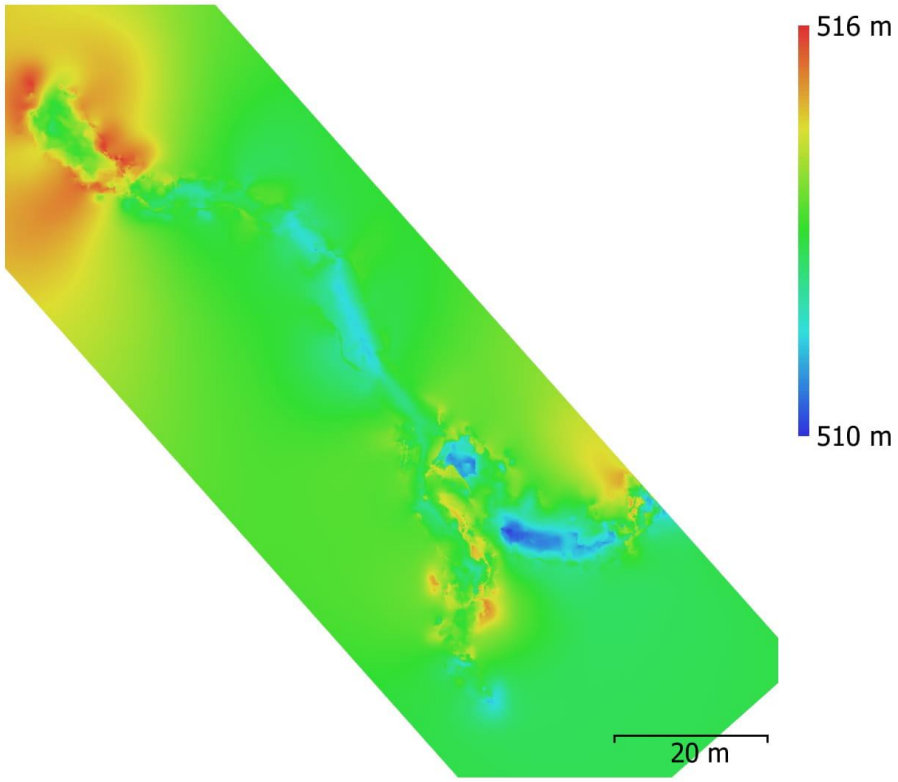

Fig. 6. Reconstructed digital elevation model.

Resolution:	9.78 mm/pix
Point density:	1.05 points/cm²

Processing Parameters

General	
Cameras	4678
Aligned cameras	2750
Markers	13
Scale bars	9
Shapes	
Polylines	35
Polygons	4512
Coordinate system	WGS 84 (EPSG::4326)
Rotation angles	Yaw, Pitch, Roll
Point Cloud	
Points	811,588 of 3,189,270
RMS reprojection error	0.205614 (1.02577 pix)
Max reprojection error	0.466359 (7.6231 pix)
Mean key point size	4.76667 pix
Point colors	3 bands, uint8
Key points	No
Average tie point multiplicity	3.6677
Dense Point Cloud	
Points	7,227,280
Point colors	3 bands, uint8
Reconstruction parameters	
Quality	Low
Depth filtering	Aggressive
Depth maps generation time	32 minutes 16 seconds
Dense cloud generation time	1 days 11 hours
Model	
Faces	506,776
Vertices	256,833
Vertex colors	3 bands, uint8
Reconstruction parameters	
Surface type	Arbitrary
Source data	Dense
Interpolation	Enabled
Quality	Low
Depth filtering	Aggressive
Face count	889,168
Processing time	10 minutes 27 seconds
DEM	
Size	12,663 x 13,466
Coordinate system	WGS 84 (EPSG::4326)
Reconstruction parameters	
Source data	Dense cloud
Interpolation	Enabled
Processing time	1 minutes 10 seconds
Orthomosaic	
Size	70,245 x 66,601
Coordinate system	WGS 84 (EPSG::4326)
Colors	3 bands, uint8
Reconstruction parameters	
Blending mode	Mosaic
Surface	Mesh
Enable hole filling	Yes
Processing time	58 minutes 30 seconds
Software	

Version	1.4.4 build 6848
Platform	Windows 64

Owl Cave

Processing Report
11 October 2018

Survey Data

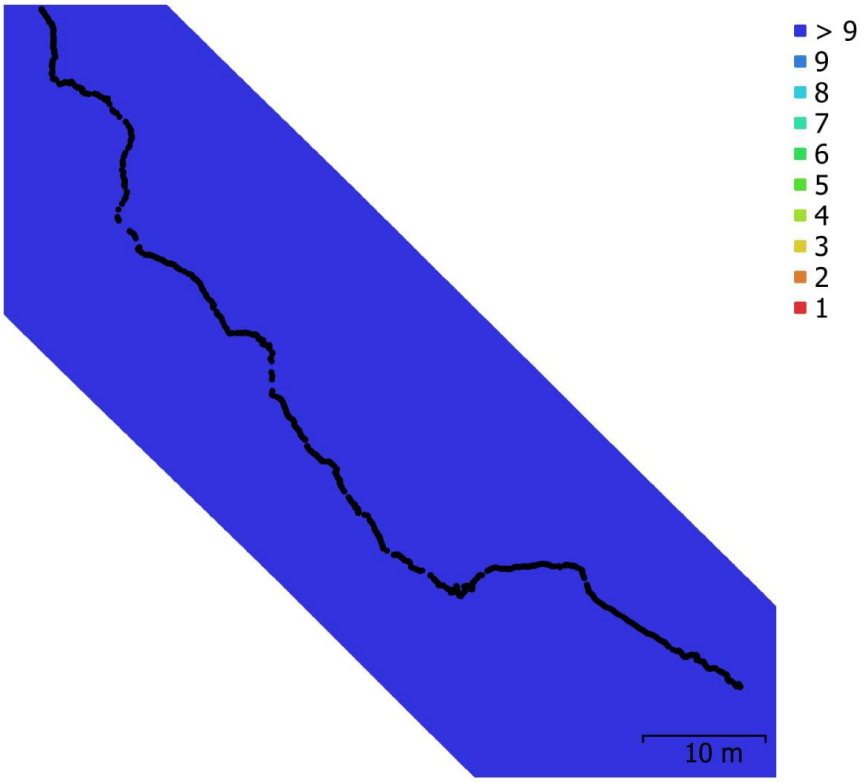

Fig. 1. Camera locations and image overlap.

Number of images:	1,748	Camera stations:	1,102
Flying altitude:	3.08 m	Tie points:	548,360
Ground resolution:	2.03 mm/pix	Projections:	1,749,050
Coverage area:	2.03e+03 m²	Reprojection error:	1.36 pix

Camera Model	Resolution	Focal Length	Pixel Size	Precalibrated
Camera	3840 x 2160	unknown	unknown	No

Table 1. Cameras.

Camera Calibration

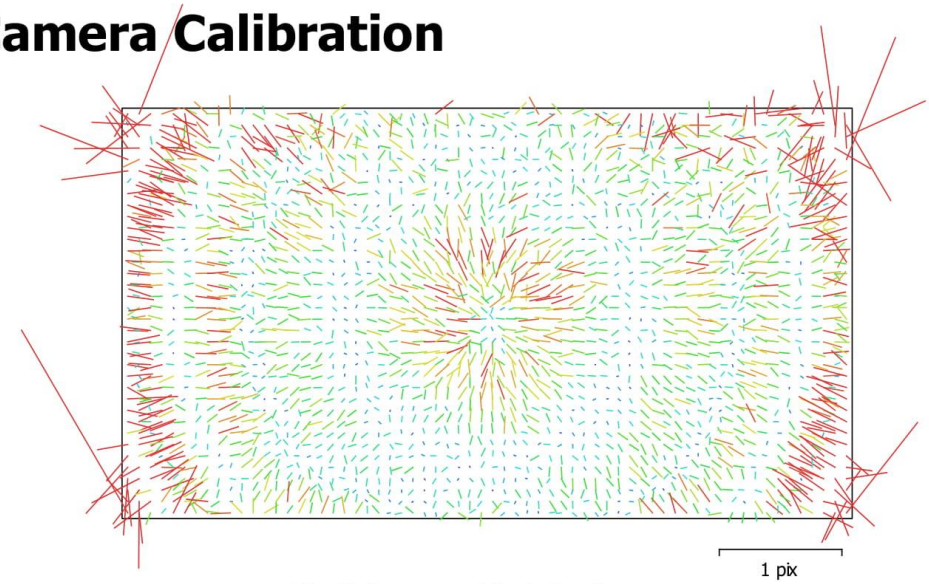

Fig. 2. Image residuals for Camera.

Camera

1748 images

Type	Resolution	Focal Length	Pixel Size
Frame	**3840 x 2160**	**unknown**	**unknown**

	Value	Error	F	Cx	Cy	B1	B2	K1	K2	K3	K4	P1	P2
F	**1760.42**	0.058	1.00	-0.03	-0.07	-0.50	0.01	-0.22	0.30	-0.34	0.36	0.05	0.07
Cx	**11.7381**	0.083		1.00	-0.03	0.07	-0.03	0.02	-0.03	0.04	-0.05	-0.18	0.01
Cy	**-10.7467**	0.1			1.00	0.04	0.08	-0.00	-0.02	0.03	-0.03	0.05	-0.40
B1	**-0.83444**	0.038				1.00	0.02	-0.03	0.02	-0.02	0.02	-0.09	-0.05
B2	**-1.74398**	0.036					1.00	0.00	0.00	-0.01	0.01	0.04	-0.09
K1	**-0.25795**	2.2e-05						1.00	-0.95	0.88	-0.82	0.05	0.01
K2	**0.0926966**	2.6e-05							1.00	-0.98	0.94	-0.03	-0.01
K3	**-0.0220923**	1.2e-05								1.00	-0.99	0.02	0.00
K4	**0.00223339**	1.7e-06									1.00	-0.01	-0.00
P1	**-9.35376e-05**	1.5e-06										1.00	-0.04
P2	**6.94741e-05**	2e-06											1.00

Table 2. Calibration coefficients and correlation matrix.

Ground Control Points

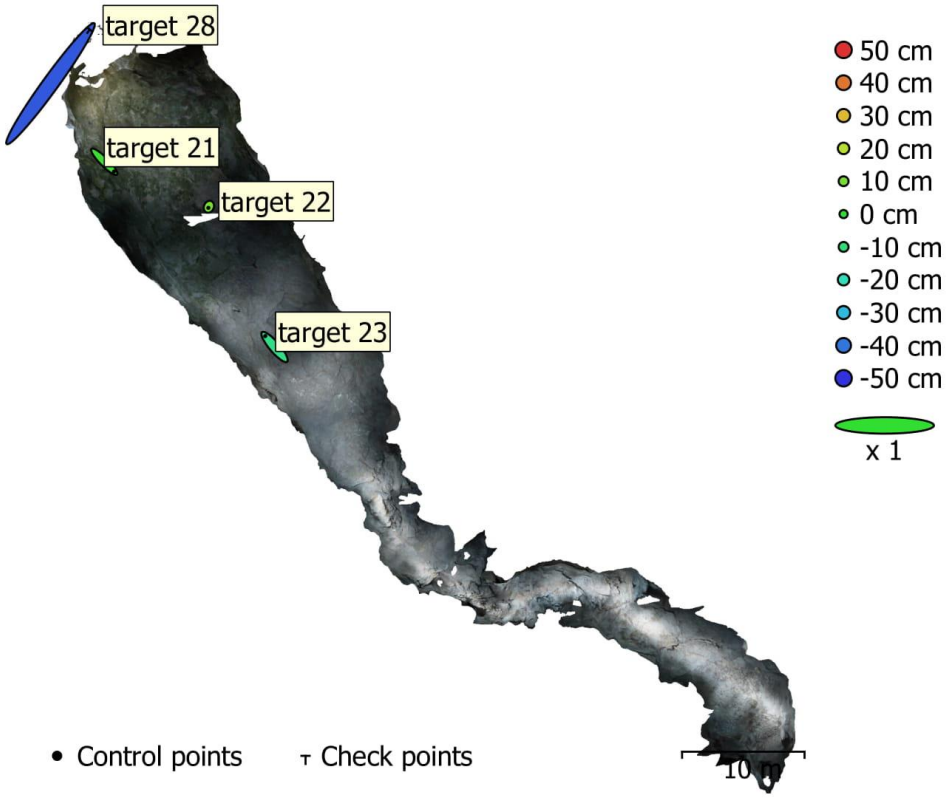

Fig. 3. GCP locations and error estimates.
Z error is represented by ellipse color. X,Y errors are represented by ellipse shape.
Estimated GCP locations are marked with a dot or crossing.

Count	X error (m)	Y error (m)	Z error (m)	XY error (m)	Total (m)
3	1.27084	1.38485	0.0932637	1.87958	1.8819

Table 3. Control points RMSE.
X - Longitude, Y - Latitude, Z - Altitude.

Count	X error (m)	Y error (m)	Z error (m)	XY error (m)	Total (m)
1	6.4085	8.84164	0.44533	10.9199	10.9289

Table 4. Check points RMSE.
X - Longitude, Y - Latitude, Z - Altitude.

Label	X error (m)	Y error (m)	Z error (m)	Total (m)	Image (pix)
target 21	1.59672	-1.60244	0.019251	2.26223	0.336 (25)
target 22	-0.0821258	-0.176734	0.103293	0.220565	0.215 (9)
target 23	-1.51289	1.77606	-0.122696	2.33629	0.284 (13)
Total	**1.27084**	**1.38485**	**0.0932637**	**1.8819**	**0.302**

Table 5. Control points.
X - Longitude, Y - Latitude, Z - Altitude.

Label	X error (m)	Y error (m)	Z error (m)	Total (m)	Image (pix)
target 28	6.4085	8.84164	-0.44533	10.9289	0.241 (7)
Total	**6.4085**	**8.84164**	**0.44533**	**10.9289**	**0.241**

Table 6. Check points.
X - Longitude, Y - Latitude, Z - Altitude.

Scale Bars

Label	Distance (m)	Error (m)
target 23_target 28	29.0789	0.178916
target 22_target 28	18.4968	0.19675
Total		**0.188045**

Table 7. Control scale bars.

Digital Elevation Model

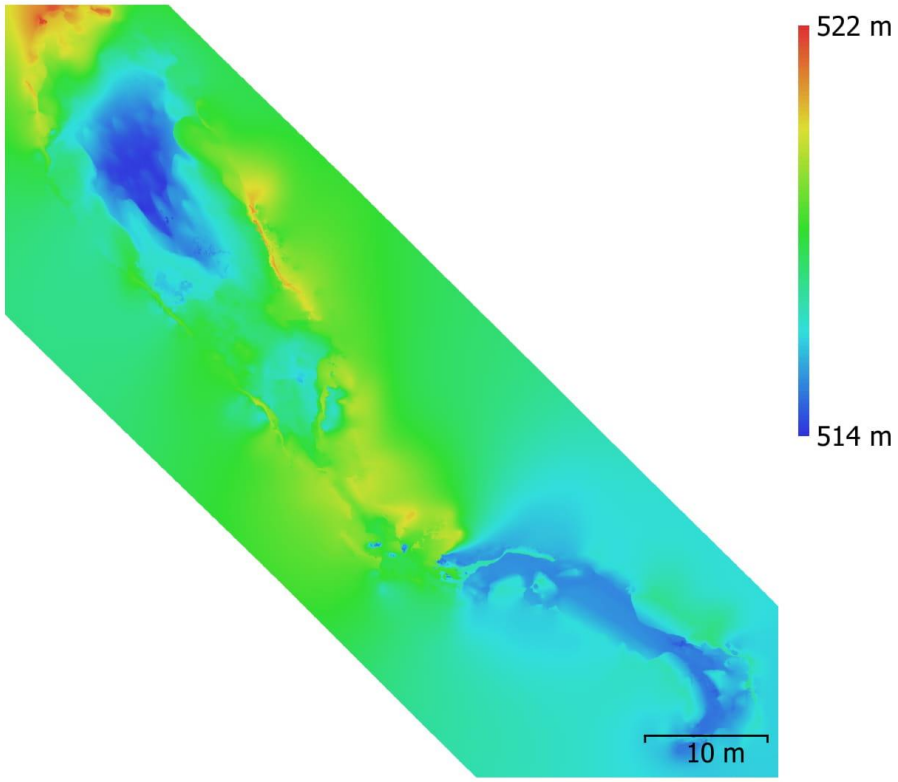

Fig. 4. Reconstructed digital elevation model.

Resolution:	1.62 cm/pix
Point density:	0.379 points/cm²

Processing Parameters

General	
Cameras	1748
Aligned cameras	1102
Markers	4
Scale bars	2
Coordinate system	WGS 84 (EPSG::4326)
Rotation angles	Yaw, Pitch, Roll
Point Cloud	
Points	548,360 of 2,120,256
RMS reprojection error	0.276605 (1.36055 pix)
Max reprojection error	0.695929 (12.1772 pix)
Mean key point size	4.73344 pix
Point colors	3 bands, uint8
Key points	No
Average tie point multiplicity	3.88444
Alignment parameters	
Accuracy	High
Generic preselection	Yes
Key point limit	0
Tie point limit	0
Adaptive camera model fitting	Yes
Matching time	3 hours 17 minutes
Alignment time	1 hours 3 minutes
Optimization parameters	
Parameters	f, b1, b2, cx, cy, k1-k4, p1, p2
Adaptive camera model fitting	Yes
Optimization time	2 minutes 18 seconds
Dense Point Cloud	
Points	3,522,704
Point colors	3 bands, uint8
Reconstruction parameters	
Quality	Low
Depth filtering	Aggressive
Depth maps generation time	21 minutes 29 seconds
Dense cloud generation time	4 hours 6 minutes
Model	
Faces	450,692
Vertices	225,420
Vertex colors	3 bands, uint8
Texture	4,096 x 4,096, 4 bands, uint8
Reconstruction parameters	
Surface type	Arbitrary
Source data	Dense
Interpolation	Enabled
Quality	Low
Depth filtering	Aggressive
Face count	450,004
Processing time	4 minutes 37 seconds
Texturing parameters	
Mapping mode	Generic
Blending mode	Mosaic
Texture size	4,096 x 4,096
Enable hole filling	Yes
Enable ghosting filter	No
UV mapping time	43 seconds

Blending time	11 minutes 20 seconds
Tiled Model	
Texture	3 bands, uint8
Reconstruction parameters	
Source data	Dense cloud
Tile size	256
Enable ghosting filter	No
Processing time	3 hours 57 minutes
DEM	
Size	5,877 x 5,789
Coordinate system	WGS 84 (EPSG::4326)
Reconstruction parameters	
Source data	Dense cloud
Interpolation	Enabled
Processing time	16 seconds
Orthomosaic	
Size	29,467 x 31,060
Coordinate system	WGS 84 (EPSG::4326)
Colors	3 bands, uint8
Reconstruction parameters	
Blending mode	Mosaic
Surface	Mesh
Enable hole filling	Yes
Processing time	18 minutes 12 seconds
Software	
Version	1.4.4 build 6848
Platform	Windows 64